Thesis

THE EFFECT OF THE POLYAMINE SPERMIDINE ON HEART FUNCTION ASSESSED BY ECHOCARDIOGRAPHY

submitted by

Katharina Melanie Waltl

in partial fulfillment of the requirements for the degree of

Doktor(in) der gesamten Heilkunde

(Dr.$^{(in)}$ med. univ.)

at the

Medical University of Graz

executed at the
University Department of Internal Medicine
Division of Cardiology

under the supervision of

Ewald Kolesnik, Dr. med. univ. Dr. scient. med.

Dirk von Lewinski, Assoc. Prof. Priv.-Doc. Dr. med.

Graz, February 20th, 2024

Declaration of Academic Integrity

I hereby confirm that the present diploma thesis is the result of my own independent scholarly work. I also confirm that in all cases, where material from the work of others (in books, articles, essays, dissertations, and on the internet) is acknowledged, quotations and paraphrases are clearly indicated. No material other than that cited in the reference list has been used. I have read and understood the Medical University's regulations and procedures concerning plagiarism.

Graz, February 20th, 2024 *Katharina Melanie Waltl m.p.*

Acknowledgement

First, I would especially like to thank my primary supervisor Dr. med. univ. Dr. scient. med. Ewald Kolesnik for his trust and the possibility of writing my thesis at the Department of Cardiology at the Medical University of Graz. During the entire process of this thesis, he supported me with his expertise with great patience and was always available to answer my questions quickly and helpfully. I would further like to show my thankfulness to my secondary supervisor Assoc. Prof. Priv.-Doc. Dr. med. Dirk von Lewinski for the cooperation.

From the bottom of my heart, I would like to thank my family, especially my parents for making my studies possible and for always supporting me unconditionally along the way. I also want to express my warmest gratitude to my brother and my grandma for their emotional and mental support, particularly in challenging times of excessive learning. Without you, I would not be where I am today!

I would further like to say a silent thank you to my grandpa, who encouraged me to study medicine and always believed in me. You are missed!

My very special thanks also go to Anja, Michaela, Viktoria, Fabienne, and Anna, who were always by my side and pushed me through my studies. You truly are the best friends anyone could wish for!

Last but not least, I want to express my deepest gratitude to my partner Paul for his acceptance, motivation, and endless support. Thank you for being my anchor!

Zusammenfassung

Hintergrund und Fragestellung: Arterielle Hypertonie ist der Hauptrisikofaktor für kardiovaskuläre Erkrankungen (CVDs) und Todesfälle mit zunehmender Inzidenz. In einer Tierstudie konnte bereits nachgewiesen werden, dass die Supplementierung mit dem Polyamin Spermidin zu reduzierten Blutdruckwerten bei Mäusen führte. Anhand konventioneller echokardiographischer Messwerte und Strainparameter soll diese Diplomarbeit die Evidenz der potenziell kardioprotektiven Effekte von Spermidin auf die Herzfunktion von Hypertoniker*innen erweitern.

Material und Methodik: Als Basis dieser Studie diente eine retrospektive Datenanalyse von Echokardiographie-Loops von 20 Patient*innen mit arterieller Hypertonie aus der SMARTEST Studie zu vier Zeitpunkten (Woche 0, 8, 12 und 20). Die Proband*innen nahmen für jeweils 8 Wochen 4mg Spermidin täglich und ein Placebo mit einer dazwischengelegenen vierwöchigen Ausschwemmphase im Crossover-Design ein. Zur Bewertung der Herzfunktion wurden Standard Echokardiographiewerte und Strainparameter der Visite 1 und Visite 4 statistisch ausgewertet und miteinander verglichen.

Ergebnisse: Die Ergebnisse dieser Studie zeigten keine signifikanten Veränderungen der linksventrikulären (LV) Funktion und Volumina, der rechtsventrikulären (RV) Funktion und des Durchmessers, der linksatrialen (LA) Funktion und des Durchmessers sowie der diastolischen Funktion zwischen Visite 1 und Visite 4. Hinsichtlich Strainanalysen wurden an Visite 4 sowohl eine stark positive Korrelation zwischen LV Endo globalen longitudinalen Strain (GLS) und LV AutoStrain ($r = 0.651$) als auch eine stark negative Korrelation zwischen biplaner linksventrikulärer Auswurffraktion (LVEF) und LV Endo GLS ($r = -0.593$) festgestellt.

Schlussfolgerung: Die Verabreichung von Spermidin führte bei Hypertoniker*innen zu keinen signifikanten Veränderungen echokardiographischer Volumina, linearer Messwerte und Strainparameter. Jedoch konnte anhand dieser Diplomarbeit durch echokardiographische Evaluierung die Sicherheit von oraler Spermidin-Supplementierung bezogen auf die Herzfunktion hypertensiver Patient*innen gezeigt werden. Für den Nachweis der potenziell kardioprotektiven Effekte von Spermidin und für das Verständnis des Stellenwertes von GLS in arterieller Hypertonie sind weitere klinische Erforschungen notwendig.

Abstract

Background and Aim: Arterial hypertension is the main risk factor for cardiovascular diseases (CVDs) and deaths with increasing incidence. In an animal study, it could already be proven that the supplementation with the polyamine spermidine led to lower blood pressure levels in mice. This thesis aims to give further insights into the possible cardioprotective effects of spermidine on heart function in patients with hypertension disease assessed by both conventional echocardiographic and strain parameters.

Material and Methods: This work was based on retrospective data analysis of echocardiographic loops of 20 patients with arterial hypertension from the SMARTEST trial at four points in time (weeks 0, 8, 12, and 20). The subjects received 4mg spermidine per day and a placebo for each eight weeks with a washout interval of four weeks in between in a crossover design. Standard echocardiographic and strain parameters of visit 1 and visit 4 were statistically evaluated and compared with each other to assess cardiac function.

Results: The results of this study showed no significant changes in left ventricular (LV) function and volumes, right ventricular (RV) function and diameter, left atrial (LA) function and diameter, and diastolic function between visit 1 and visit 4. Regarding strain analyses, a strong positive correlation between LV Endo global longitudinal strain (GLS) and LV AutoStrain ($r = 0.651$) as well as a strong negative correlation between biplane left ventricular ejection fraction (LVEF) and Endo GLS ($r = -0.593$) were determined on visit 4.

Conclusion: The administration of spermidine in hypertensive patients did not lead to any significant echocardiographic changes in volume, linear, and strain parameters. Nevertheless, this work could show the safety of oral spermidine supplementation on cardiac function in hypertensive patients evaluated by echocardiography. Further clinical research is necessary for the proof of the possible cardioprotective effects of spermidine and the understanding of the importance of GLS in hypertension disease.

Table of Contents

List of Abbreviations and Definitions

ABPM	*ambulatory blood pressure monitoring*
ACE	*angiotensin-converting enzyme*
ARB	*angiotensin receptor blocker*
A2C	*apical two chamber view*
A3C	*apical three chamber view*
A4C	*apical four chamber view*
A5C	*apical five chamber view*
BSA	*body surface area*
CCB	*calcium channel blocker*
CMR	*cardiac magnetic resonance*
CVD	*cardiovascular disease*
DBP	*diastolic blood pressure*
DICOM	*Digital Imaging and Communications in Medicine*
DNA	*deoxyribonucleic acid*
ECG	*electrocardiogram*
ED	*end-diastolic*
EDV	*end-diastolic volume*
EF	*ejection fraction*
e.g.	*exempli gratia meaning for example*
ES	*end-systolic*
ESC	*European Society of Cardiology*
ESH	*European Society of Hypertension*
ESV	*end-systolic volume*
GCS	*global circumferential strain*
GE	*General Electric*
GLS	*global longitudinal strain*
GRS	*global radial strain*
HBPM	*home blood pressure monitoring*

HFpEF	*heart failure with preserved ejection fraction*
IBM	*International Business Machines Corporation*
ISCV	*IntelliSpace Cardiovascular*
LA	*left atrial*
LAV	*left atrial volume*
LV	*left ventricular*
LVEF	*left ventricular ejection fraction*
LVH	*left ventricular hypertrophy*
LVLd	*left ventricular length in diastole*
LVLs	*left ventricular length in systole*
LVOT	*left ventricular outflow tract*
MRI	*magnetic resonance imaging*
NT-proBNP	*N-terminal pro B-type natriuretic peptide*
NYHA	*New York Heart Association*
PLAX	*parasternal long axis view*
PSAX	*parasternal short axis view*
RAS	*renin-angiotensin system*
RNA	*ribonucleic acid*
RV	*right ventricular*
SBP	*systolic blood pressure*
SMARTEST	*Spermidine Anti-Hypertension Study*
SPSS	*Statistical Package for the Social Sciences*
SR	*strain rate*
STE	*speckle tracking echocardiography*
SV	*stroke volume*
TAPSE	*Tricuspid Annular Plane Systolic Excursion*
TDI	*tissue Doppler imaging*
TTE	*transthoracic echocardiography*
UK	*United Kingdom*

US	*United States*
VTI	*velocity time integral*
V1	*visit 1*
V2	*visit 2*
V3	*visit 3*
V4	*visit 4*
WHO	*World Health Organization*
2D	*two-dimensional*
2D CPA	*2D Cardiac Performance Analysis*
3D	*three-dimensional*

List of Figures

List of Tables

1 Introduction

1.1 Arterial Hypertension

1.1.1 Definition

In reference to the 2018 guidelines of the European Society of Cardiology (ESC) and the European Society of Hypertension (ESH) for the management of arterial hypertension, *"hypertension is defined as office systolic blood pressure (SBP) values ≥ 140 mmHg and/or diastolic blood pressure (DBP) values ≥ 90 mmHg"* [1]. Hypertension disease can be classified into grades I-III, as listed in Table 1.

Table 1: *Classification of arterial hypertension. Adapted from [1].*

Category	SBP [mmHg]		DBP [mmHg]
optimal	< 120	and	< 80
normal	120 - 129	and/or	80 - 84
high normal	130 - 139	and/or	85 - 89
grade I hypertension	140 - 159	and/or	90 - 99
grade II hypertension	160 - 179	and/or	100 - 109
grade III hypertension	≥ 180	and/or	≥ 110
isolated systolic hypertension	≥ 140	and	< 90

1.1.2 Scope of the Problem

Arterial hypertension represents the most common risk factor for CVDs and cause of deaths worldwide [2,3]. In reference to Statistik Austria hospital discharge statistics, there were 14437 hospitalizations in acute care hospitals due to the diagnosis of arterial hypertension in 2021 [4]. The prevalence increases with age [2] and more than 60% of people older than 60 years suffer from hypertension [1]. The Framingham Heart Study has demonstrated that the cumulative lifetime risk of developing hypertension disease is up to 90% for both genders at the age of 55 and 65 years [5]. In 2015 the worldwide prevalence of this disease was estimated to be 1.13 billion [6]. Due to the elderly population, physical inactivity, higher body weights, and

unhealthy lifestyle factors [1], a further rise of close to 1.56 billion adult people with hypertension disease all over the world is expected by 2025 [7].

High blood pressure causes at least 7.6 million deaths every year, this corresponds to 13.5% of all cases of deaths globally [8]. In 2015, approximately 10.7 million deaths were caused by arterial hypertension [1,9]. Possible impacts of high blood pressure include coronary artery disease, myocardial infarction, heart failure, chronic kidney disease, peripheral artery disease, and dementia [1,10,11]. In addition, hypertension disease represents the main risk factor for ischemic and hemorrhagic strokes [12]. For instance, in 2015 an estimated number of 3.5 million strokes and 4.9 million ischemic heart diseases occurred due to elevated SBP [9]. Furthermore, a quarter of all myocardial infarctions in Europe have been associated with hypertension disease over the last few years, and approximately 40% of all deaths Europe-wide are caused by CVDs due to hypertension per year [11,13]. In younger patients, the association between arterial hypertension, higher risk for CVD, and all-cause mortality is particularly strong [14].

According to the World Health Organization (WHO), less than 14% of all adults with hypertension have stable blood pressure levels < 140/90 mmHg, even though multiple efficient and inexpensive antihypertensive therapy strategies are widely available [15]. In addition, the EURIKA study, including 5559 patients with arterial hypertension Europe-wide, from whom 94% received antihypertensive drug therapy, has shown that only 38.8% of all treated participants could achieve the target blood pressure ranges [16].

1.1.3 Etiology

Depending on the etiology, arterial hypertension can be classified into primary and secondary hypertension.

1.1.3.1 Primary Hypertension

Primary hypertension, also known as essential hypertension, is defined as lasting increased blood pressure levels without an identifiable cause and represents the leading type of arterial hypertension with more than 90% of all cases [17].

Although the cause of primary hypertension is still unclear, several risk factors are described, e.g. higher age, metabolic syndrome, and obesity [18-20]. Both in developed and developing countries, 25-35% of adults suffer from primary hypertension, whereby approximately 60-70% of the affected are older than 70 years [18]. Furthermore, metabolic syndrome is present in 15-20% of adults with primary hypertension disease [19,20]. In addition, the prevalence of primary hypertension among normal-weight children is about 5%, among overweight children about 20%, among obese children about 26%, and in severely obese children the prevalence is up to 39% [19].

1.1.3.2 Secondary Hypertension

Secondary hypertension is caused by an underlying, identifiable, and potentially reversible disease [21]. It is estimated that 5-10% of all patients with hypertension suffer from secondary hypertension, whereby especially children and young adults are affected [22-24].

Table 2: *Overview of the most common underlying causes of secondary hypertension. Adapted from [1,22].*

Secondary cause	Prevalence in hypertensive patients	Prevalence in patients with resistant hypertension
Obstructive sleep apnea	5 - 10%	> 30%
Renal parenchymal disease	2 - 10%	2 - 10%
Renal artery stenosis	1 - 10%	2.5 - 20%
Primary aldosteronism	5 - 15%	6 - 23%
Thyroid disease	1 - 2%	1 - 3%
Cushing's syndrome	< 1%	< 1%
Phaeochromocytoma	< 1%	< 1%
Coarctation of the aorta	< 1%	< 1%

The underlying disease is strongly age-dependent: In childhood, secondary hypertension is mainly caused by renal parenchymal disease and coarctation of the aorta. However, in patients ≥ 65 years secondary hypertension often occurs with atherosclerotic renal artery stenosis, renal failure, and hypothyroidism [21]. The most common underlying causes are summarized in Table 2.

Especially in cases of patients younger than 40 years, with underlying treatment-resistant or severe manifestations (grade III), hypertensive emergencies, acute rise of blood pressure in previously stable values, and coexisting organ damages, e.g. left ventricular hypertrophy (LVH), screening for secondary hypertension should be considered [1,22,25].

1.1.4 Diagnostic Tools

1.1.4.1 Blood Pressure Measurements

Correct blood pressure measurements are necessary for the diagnosis of arterial hypertension. There are both in-office and out-of-office blood pressure measurements available.

High blood pressure should initially be diagnosed by repeated office blood pressure measurements on both upper arms after a few minutes of rest, twice or three times in one to four weekly intervals [1,10,26,27]. Office blood pressure measurements can be performed with auscultatory- or oscillometric-, semiautomatic- as well as automatic devices [1].

In addition, for a more accurate diagnosis and confirmation of the disease, also out-of-office blood pressure measurements, e.g. home blood pressure monitoring (HBPM) or ambulatory blood pressure monitoring (ABPM), are of great importance [1]. The limit blood pressure values of 24-hour measurements are ≥ 130/80 mmHg by ABPM and ≥ 135/85 mmHg by HBPM [1,28]. Out-of-office measurements should be performed in adults with high in-office blood pressure to detect white-coat hypertension or in patients with suspected hypertension to exclude masked hypertension [29].

In specific clinical situations, e.g. blood pressure of at minimum 180/110 mmHg, cardiovascular high-risk patients, and co-existing end-organ damage, it is indicated

to diagnose hypertension disease by one-time measurement already and to start antihypertensive therapy immediately [10].

1.1.4.2 Electrocardiogram

A 12-lead electrocardiogram (ECG) is usually part of the routine diagnosis of hypertension disease [1]. Arterial hypertension affects mostly the LV geometry and the hypertension-induced chronic pressure overload results primarily in LVH, whereby these ventricular changes can still be missing in the early stages of the disease [30,31]. However, the ECG has a low sensitivity for the detection of LVH [1,31], which represents a main risk factor for cardiovascular morbidity and mortality [31].The ECG diagnostic index Sokolow Lyon criteria for LVH shows a sensitivity of only 21% and a specificity of 89% [31,32]. Furthermore, the sensitivity for LVH varies depending on the patient's body weight [1].

Nevertheless, this diagnostic tool continues to be used because of its low costs and widespread availability [33].

1.1.4.3 Transthoracic Echocardiography

In the management of arterial hypertension, two-dimensional (2D) transthoracic echocardiography (TTE) is especially useful for the evaluation of LVH. Compared to ECG, TTE allows the detection of arterial hypertension based on determined LVH with higher sensitivity and specificity [30]. Furthermore, 2D TTE provides additional cardiovascular risk criteria, e.g. LV geometry, LV systolic and diastolic function, left atrial volume (LAV), and wall motion disorders [30,34-38].

Table 3: *Criteria of echocardiographically determined left ventricular hypertrophy. Adapted from [1]. BSA = body surface area.*

Parameter	Calculation	Unit	Threshold values	
			Men	Women
LVH	LV mass/height$^{2.7}$	[g/m$^{2.7}$]	> 50	> 47
LVH	LV mass/BSA	[g/m^2]	> 115	> 95

In reference to the 2018 ESC/ESH guidelines, a 2D TTE is recommended for hypertensive patients with ECG alterations as well as clinical signs of LV dysfunction [1].

1.1.5 Therapy

The routine treatment of hypertension disease is based on both non-drug and drug therapy strategies.

1.1.5.1 Non-Drug Therapy

A healthy lifestyle can prevent arterial hypertension or at least delay the onset of disease. Furthermore, healthy lifestyle factors can reduce the risk of CVDs [39,40]. For this reason, especially patients with arterial hypertension grade I can benefit greatly from healthy lifestyle modifications, and the need for pharmacological therapy can be avoided or at least be delayed [1,39]. Moreover, lifestyle modifications can amplify the effect of pharmacological antihypertensive treatment [1]. Salt restriction to < 5g daily [1,41-44], a balanced diet as well as rare consumption of alcohol are highly recommended [1,45,46]. In addition, doing sports regularly, losing body weight, and becoming a non-smoker is highly advisable [1,39,45,47,48]. Besides that, stress reduction may have a positive effect on hypertension disease in patients with high levels of stress [47,48].

Due to their great benefits, lifestyle modifications should be applied for all patients with prehypertension and hypertension disease [1].

1.1.5.2 Drug Therapy

In most patients, additional drug therapy is indicated to achieve controlled blood pressure levels. Especially for all patients with hypertension disease grade II and III, an additional pharmacological therapy is indicated [49]. According to the 2018 ESC/ESH guidelines, there are five different groups of medications highly recommended for antihypertensive basic therapy: angiotensin-converting enzyme (ACE) inhibitors, angiotensin receptor blockers (ARBs), beta-blockers, calcium channel blockers (CCBs) and diuretics, e.g. thiazides or thiazide-like diuretics [1].

In general, the start of drug therapy is strongly suggested for adults with confirmed hypertension disease and SBP of > 140 mmHg or DBP of > 90 mmHg [15].

Indications for an antihypertensive monotherapy include low-risk patients with grade I hypertension (SBP < 150mmHg), very high-risk patients with high-normal blood pressure as well as elderly and rather fragile patients [1].

A double drug combination is initially necessary for most patients with hypertension disease. It is highly advocated to combine a renin-angiotensin system (RAS) blocker, either an ACE inhibitor or an ARB, with a CCB or a diuretic. In special circumstances, e.g. post-myocardial infarction, heart failure, angina pectoris, or control of heart rate, the patient should be treated with a combination of a beta-blocker and one of the other five major groups of pharmacological therapy [1]. Furthermore, other double-drug strategies can be applied [1], but the combination of an ACE inhibitor and an ARB is not suggested [1,48,50].

If blood pressure cannot be controlled sufficiently by a double combination, a triple drug treatment should be implemented [1,48]. A triple drug combination typically consists of a RAS blocker with a CCB and a thiazide or a thiazide-like diuretics. If the blood pressure range is still not satisfying, there is an urgent suspicion of resistant hypertension and spironolactone should be applied additionally. Moreover, when spironolactone is not tolerated well, other drugs like a diuretic, e.g. amiloride, a beta-blocker, or an alpha-blocker are indicated [1].

Figure 1 summarizes the current recommendations of antihypertensive therapy strategies for patients with uncomplicated hypertension disease.

1.1.5.3 Therapy Targets

The main target of lowering blood pressure levels is to prevent CVD and hypertension-induced end-point events, e.g. myocardial infarction and stroke, without reducing quality of life [50]. The in-office blood pressure level should initially be decreased to < 140/90 mmHg [1]. If antihypertensive treatment is tolerated well, it is suggested to further improve blood pressure levels to ≤ 130/80 mmHg in most patients [1,51].

In addition, for patients < 65 years in-office SBP target values of 120-129 mmHg, and for patients > 65 years of 130-139 mmHg are highly advisable [1,52]. Moreover, the recommended in-office DBP target range is 70-79 mmHg for all ages [1].

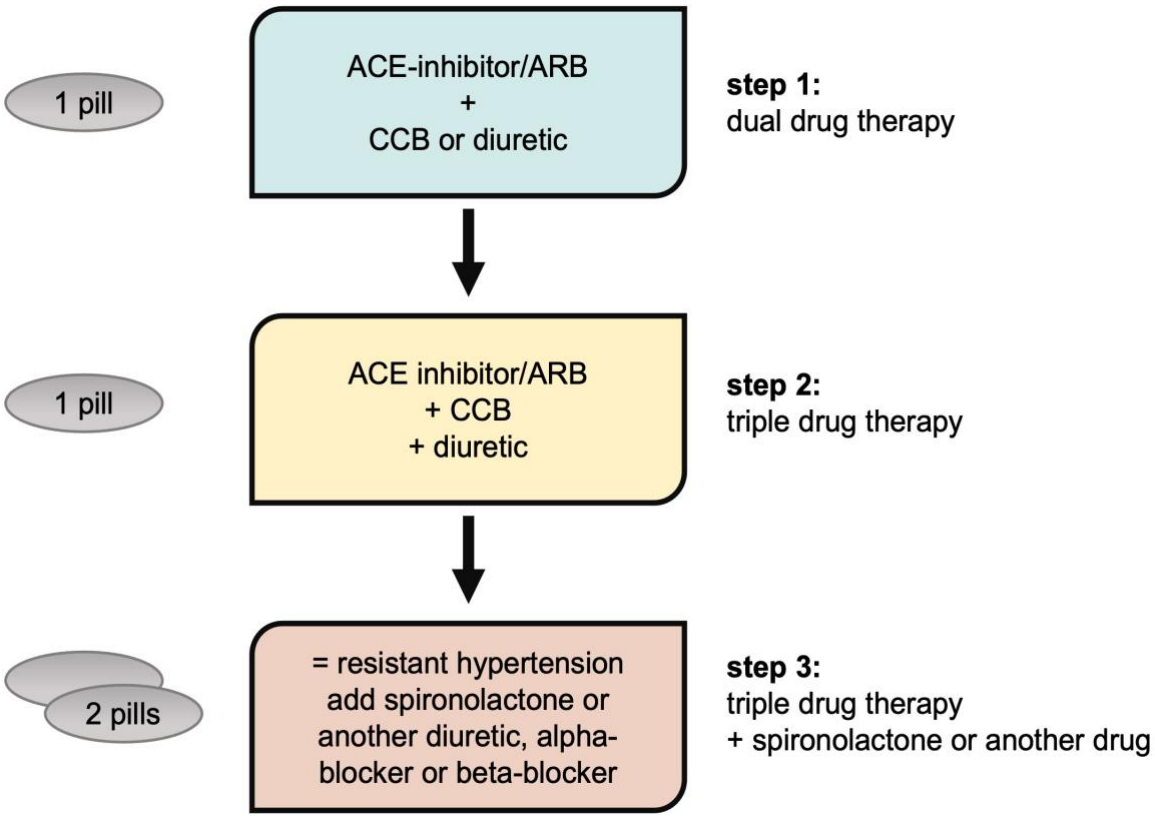

Figure 1: *Pharmacological algorithm of antihypertensive therapy for uncomplicated arterial hypertension. Adapted from [1].*

1.2 Polyamine

Polyamines are defined as a group of positively charged molecules that have amino groups at both ends of a hydrocarbon chain [53]. Due to their positive charge in physiological conditions, they can interact with negatively charged macromolecules like deoxyribonucleic acid (DNA), ribonucleic acid (RNA), proteins as well as phospholipids [53-55]. Polyamines exist in nearly all cells of various organisms [53], but in mammalian cells only putrescine, spermidine, and spermine are present [56]. These polyamines are involved in various cellular processes in mammals and play an essential role in cellular proliferation [54,55], especially for the regulation of

translation [54,57]. Moreover, polyamines interact with different types of ion channels, e.g. Kir channel blocking by intracellular spermine [58].

1.2.1 Spermidine

The polyamine spermidine is a naturally occurring autophagy inducer with a molecular weight of 145.25 g/mol [59] and represents the precursor of spermine [58]. Spermine was first discovered as crystals in the human seminal fluid by the researcher Leeuwenhoek in 1678 [60].

Spermidine is the polyamine most easily absorbed by the human gut [61] and high amounts are contained in various human diets, e.g. soybeans, cauliflower, broccoli, mushrooms, green peas, cheese, chicken, and turkey [62]. In mammals, the level of spermidine decreases progressively with age [63,64] and depletion of spermidine and spermine leads to inhibition of protein synthesis and total arrest of cell growth [65]. Spermidine shows antioxidative, anti-inflammatory as well as improving mitochondrial metabolic characteristics and can enhance chaperone activity and proteostasis [66].

1.3 Strain Imaging

1.3.1 Myocardial Strain

Strain is defined as a dimensionless parameter that measures the myocardial deformation, determined by myofiber architecture, within the cardiac cycle [67]. The deformation is caused by different movement speeds of various parts of the object [68]. Due to the three-dimensional (3D) shape of the heart, there are theoretically nine different strain types, including longitudinal, radial, and circumferential strain [68,69]. The longitudinal strain represents the myocardial shortening from base to apex and is generally used both in clinical practice and research [70]. The radial strain describes the modification of wall thickness [70] and is perpendicular to the longitudinal axis and epicardium [67,68]. The circumferential strain is vertical to the radial and longitudinal axes [68] and demonstrates the change in length of the myocardium in the short axis view [70]. The remaining six strain components are shear strains due to relative movements of superimposed layers of

a volume during myocardial contraction [68] and are hardly ever used in clinical routine [67].

Strain assessment is mostly performed by echocardiography or cardiac magnetic resonance (CMR) [67]. The measurement unit is usually a percentage (%) [68], whereby a positive number displays elongation and a negative number indicates shortening of the object [70,71].

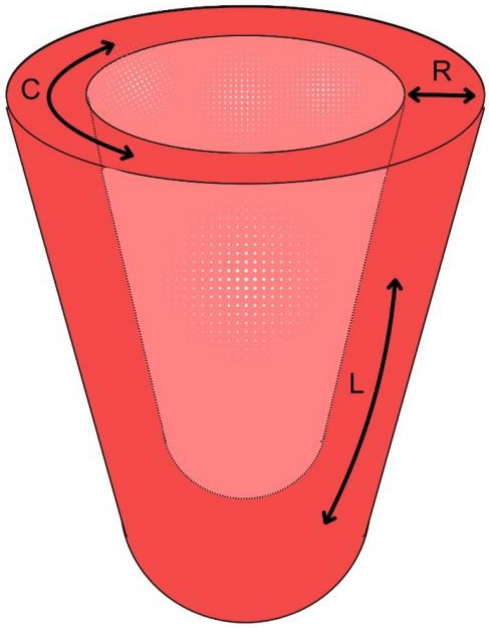

Figure 2: *The three directions of strain. Adapted from [67].*
C = circumferential strain, L = longitudinal strain, R = radial strain.

The myocardial deformation can be calculated with the Lagrangian as well as the Natural strain.

1.3.1.1 Lagrangian Strain

The Lagrangian strain describes the fractional change in the length (L) of elements at the time t [L(t)] related to their original length at the time t0 [L(t0)] [68,70]. The reference value at the time t0 generally corresponds to the end-diastolic (ED) length [70,71]. It is recommended to determine the Lagrangian strain using speckle tracking software [69].

$$S_{L(t)} = \frac{L_{(t)} - L_{(t0)}}{L_{(t0)}}$$

Figure 3: *Calculation of the Lagrangian strain.*

1.3.1.2 Natural Strain

In contrast to the Lagrangian strain, the calculation of the Natural strain includes a reference length, that is constantly changing during deformation [70].

$$S_{N(t)} = \int_{t(0)}^{t} dSR_N(t)$$

Figure 4: *Calculation of the Natural strain.*

The Lagrangian strain and the Natural strain have a nonlinear correlation and both results are almost ident in minor deformations around 5-10% [69,72]. Significant differences are apparent in case of large myocardial deformations, e.g. ventricular ejection [69], and in such cases the Natural strain is more appropriate [72].

Moreover, the Lagrangian and the Natural strain values can be converted into one another [69].

1.3.1.3 Strain Rate

Strain rate (SR) mathematically describes the changes of deformation or strain per time unit and is specified in s^{-1} [68]. SR corresponds with the shortening rate per fiber length too [71]. SR can be calculated by means of the Lagrangian as well as the Natural strain method. The Lagrangian SR represents the derivation of the Lagrangian strain [69].

$$SR_{L(t)} = \frac{dS_{L(t)}}{dt} = \frac{1}{L_0}\frac{dL_{(t)}}{dt}$$

Figure 5: *Calculation of the Lagrangian strain rate.*

However, the Natural SR describes the temporal derivation from the Natural strain and should be calculated based on tissue Doppler imaging (TDI). Furthermore, the Natural SR can also be determined via speckle tracking modality by converting the Lagrangian SR value [69].

$$SR_{N(t)} = \frac{dS_{N(t)}}{dt} = \frac{1}{L_{(t)}} \frac{dL_{(t)}}{dt}$$

Figure 6: *Calculation of the Natural strain rate.*

1.3.2 Displacement and Velocity

Displacement and velocity are further basic parameters describing myocardial function.

In detail, displacement specifies the distance by which a particular feature, e.g. a speckle or heart structure, has moved within two consecutive frames, and its measurement unit is centimeters (cm) [73].

$$X_{(t)} = \int_{ED}^{t} V(t')dt'$$

Figure 7: *Calculation of the displacement.*

Velocity defines how fast the location of a particular object changes and is specified in centimeters per second (cm/s) [73].

1.3.3 Methods of Strain Assessment

As already mentioned, echocardiography and CMR represent the most frequently applied imaging modalities for the assessment of strain in clinical practice [67]. The echocardiographic quantification of strain and SR can be performed via TDI or speckle tracking techniques [72].

1.3.3.1 Tissue Doppler Imaging

TDI enables the assessment of myocardial strain based on the measurements of regional myocardial tissue velocities [71,74]. Tissue velocity describes the speed of motion at a certain point of the heart muscle either toward or away from the transducer [74]. There are three different techniques of TDI available: pulsed wave, M-mode, and 2D color Doppler modality [75].

It should be considered, that TDI only provides a one-dimensional assessment of myocardial strain [67,72], although myocardial deformation is a 3D movement [72]. A further limitation of strain analysis via TDI is represented by the strong angle dependency between the transducer and the axis of myocardial motion [71,73]. For this reason, angle deviations of less than 15 to 20 degrees are required for valid results [76]. In addition, TDI can be influenced by cardiac translation, pathological tethering as well as the geometry of the left ventricle [77]. Furthermore, TDI is sensitive to aliasing and reverberation artifacts [78].

1.3.3.2 Speckle Tracking Echocardiography

Speckle tracking echocardiography (STE) represents a further modality for the assessment of strain using B-mode images. Since the myocardial tissue is an inhomogeneous medium with different acoustic reflections, a unique interference pattern including light and dark grey scaled pixels, defined as speckles, is created [68]. Speckle tracking algorithms enable frame-by-frame tracking of a certain myocardial area with a unique speckle pattern, also called Kernel region, during a heart circle [79].

STE allows angle-independent 2D and 3D strain analyses [78] based on the Lagrangian method of calculation [72]. For valid tracking of ultrasound speckles, high-quality ultrasound images are mandatory [78] and frame rates of 50 to 70 frames per second are considered ideal [80].

STE does not have to be preferred to TDI, as both techniques provide comparable strain analyses of similar importance [69].

1.3.3.3 Magnetic Resonance Imaging Myocardial Tagging

Magnetic resonance imaging (MRI) myocardial tagging represents a further non-invasive modality for 3D strain analysis [81]. In fact, it is mentioned as the gold standard of all non-invasive techniques for the assessment of strain [72,82].

MRI tags are radiofrequency markers that move with the myocardium during the cardiac cycle [82] and thereby provide the detection of changes in myocardial position, shape, and orientation [81]. The main disadvantages of MRI tagging include limited time resolution, low sampling rates, extensive acquisition and post-processing times, high costs as well as limited availability [72].

1.3.4 Strain Analysis

1.3.4.1 Segmental Analysis

Segments are defined as the anatomical units of the LV myocardium and the segmental strain or SR corresponds to the average value of a segment [69]. There are several left ventricle segmentation models with subdivisions into 16 to 18 segments available [69], whereby the use of the 17-segment model is recommended (see Figure 8) [83,84].

In all segment models, the rings represent, from outside to inside, the basal segments, the midpapillary muscle segments, and the apical segments [84]. The apical region of the 16-segment and 17-segment model is further subdivided into the septal, inferior, lateral, and anterior apical segments, and in the 17-segment model also segment 17, which represents the apex. The apex, also called the apical cap, corresponds to the muscle at the outermost tip of the left ventricle without an existing cavity [83]. Segmentation models allow the detection of coronary perfusion areas, provide comparable myocardial masses of the segments, and enable comparison of the results with other imaging modalities [69]. The results of the segmental analysis are color-visualized by the so-called bull's-eye plot.

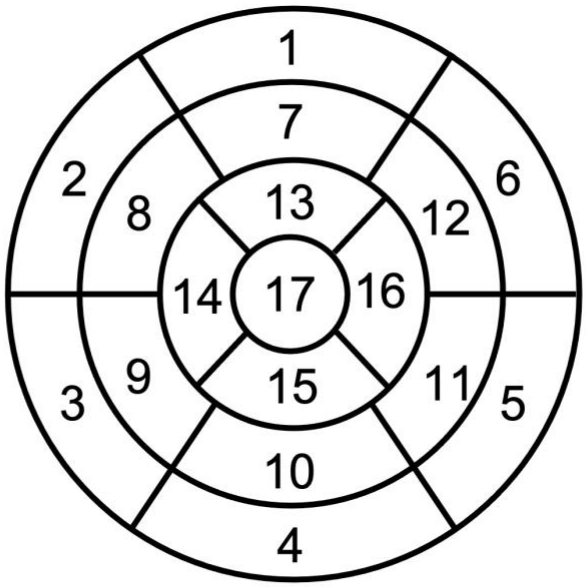

basal:	mid cavity:	apical:
1. basal anterior	7. mid anterior	13. apical anterior
2. basal anteroseptal	8. mid anteroseptal	14. apical septal
3. basal inferoseptal	9. mid inferoseptal	15. apical inferior
4. basal inferior	10. mid inferior	16. apical lateral
5. basal inferolateral	11. mid inferolateral	17. apex
6. basal anterolateral	12. mid anterolateral	

Figure 8: *17-segment model of the left ventricle and recommended topographic cardiac nomenclature. Adapted from [69].*

1.3.4.2 Layer-Specific Analysis

Layer-specific analysis enables the evaluation of myocardial deformation of a certain layer within the ventricular wall [85]. The ventricular wall is usually subdivided into endocardial, mid-myocardial, and subendocardial layers [67]. Due to mechanical layer interdependence [86] the clinical usability is questionable [67].

1.3.4.3 Global Analysis

The calculation of the LV global strain or SR includes the total myocardial line length during cardiac deformation. Otherwise, LV global strain can also be calculated by taking the average value at a series of points within the cardiac muscle line or by determining the average segmental values. By means of global analysis, GLS can

be calculated as an endocardial strain, midline strain, or epicardial strain as well as an average value over the total myocardial wall [69].

1.3.5 Analysis Results and Interpretation

Using speckle tracking software, strain analysis results are automatically visualized as strain and SR curves as well as bull's-eye plots.

Strain curves include values of peak strain, time to peak strain, and post-systolic index. SR curves offer values of peak systolic, peak early diastolic, and peak late diastolic SRs as well [70].

Bull's-eye plots enable a color-coded visualization of regional values of peak, time to peak, and post-systolic strain [70].

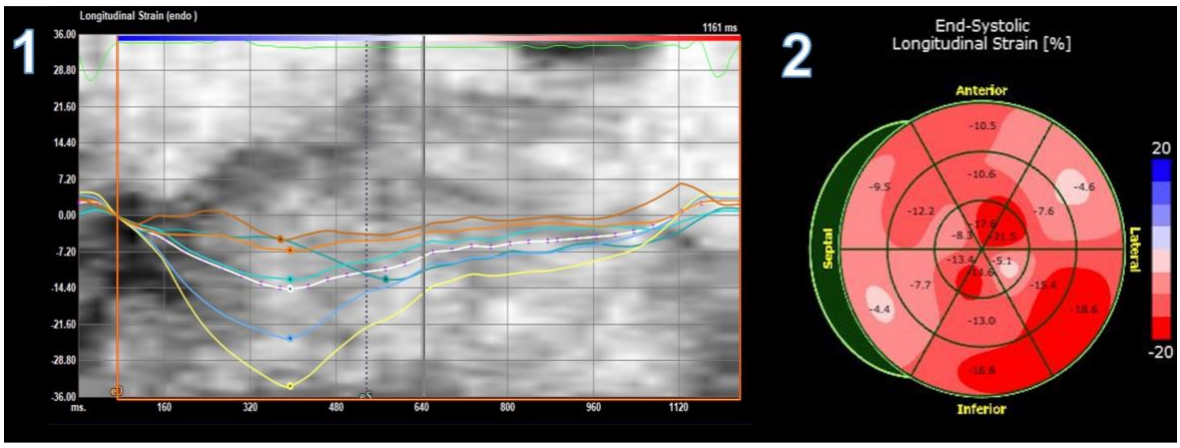

Figure 9: *Example of a longitudinal strain curve and a bull's-eye plot.*
1: Longitudinal strain [%] curve. The speckle tracking software 2D CPA by TOMTEC Imaging Systems was used.
2: Bull's-eye plot of the end-systolic longitudinal strain [%]. The speckle tracking software AutoStrain by TOMTEC Imaging Systems was used.

1.3.5.1 Standard Values of Left Ventricular Strain

In general, a standard longitudinal or circumferential strain is a negative number, and a standard radial strain is a positive number [72].

GLS represents the most frequently used strain parameter both in clinical practice and research [70,84]. However, normal values of LV GLS depend on the position of measurement, the vendor, and the strain analysis software used [84]. Therefore, different standard values for LV GLS are reported in several studies [87-90]. In an

extensive meta-analysis including data from 2597 subjects, a standard mean value of -19.7% (range of -15.9% to -22.1%) was determined for the LV GLS of healthy adults [88]. In addition, it is reported that GLS is more negative in the female population [89,91] and that LV strain decreases with age [89,92]. Furthermore, in this meta-analysis are standard average values of -23.3% (range of −20.9% to −27.8%) for the LV global circumferential strain (GCS) and 47.3% (range of 35.1% to 59.0%) for the LV global radial strain (GRS) listed for the healthy adult population [88]. However, internationally standardized strain values are still missing.

1.3.6 Influencing Factors of Strain

Strain values represent the myocardial contraction and disregard other factors affecting myofiber shortening. However, the value of strain is also influenced by further criteria such as hemodynamic and geometric aspects as well as myocardial tissue properties [67].

Strain and SR values depend on the hemodynamic factors loading conditions and heart rate [67,93-95]. An increase in the afterload results in a reduction of strain [67]. For instance, an experimental study on pigs reported a significant decrease in LV myofiber shortening on the grounds of a moderate to severe increase of 20 to 40 mmHg of LV afterload [95]. Furthermore, various studies showed decreased LV GLS values due to chronically increased afterload conditions, e.g. in patients with hypertension disease and severe aortic stenosis [96,97]. In addition, an increased heart rate leads to lower strain values because of a shortened ventricular filling time and reduced stroke volume (SV) [67]. Moreover, an increase in preload results in an increased strain value, and this fact agrees with the Frank-Starling mechanism [67], which describes how pre-stretching of the myocardial filaments strengthens the contractility of the heart muscle [67,98]. In patients with chronically increased preload conditions, e.g. due to mitral regurgitation, strain values first normalize because of LV reverse remodeling and then gradually decrease due to ventricular failure over time [67,99]. In cases with severe mitral regurgitation, adaptive LV remodeling is particularly more present when LV GLS values are ≤ 18.1% and associated with LV failure [99], even though this value is within the reported standard range of GLS [84].

The influences of the above-listed hemodynamic factors also implicate that pathological strain values are not always equivalent to myocardial dysfunction and that even standard values do not exclude any disease with certainty [67].

The myocardial deformation is also mainly affected by the SV [93] and ventricular chamber size [100]. While a higher SV, e.g. due to regurgitation, without modified chamber geometry leads to increased myocardial deformation [93], a dilated ventricle without changed SV and preserved myocardial contraction results in decreased strain indices [100]. For instance, in patients with significant mitral or aortic regurgitation and preserved LVEF, volume overload initially results in increased strain values [67,100-102]. Therefore, those values rather mirror the elevated SV instead of the increased contractility [67]. Due to persistent volume overload, patients develop chamber dilatation as well as increased wall stress in later stages, resulting in myocardial dysfunction and decreasing strain indices [102,103]. In contrast, chronic pressure overload caused, e.g. by aortic stenosis or arterial hypertension, leads to adaptive increased wall thickness and decreased chamber size [67]. In such cases, strain indices, especially LV GLS, are reduced primarily because of wall hypertrophy [96,97,104].

Furthermore, myocardial tissue factors such as fibrosis and deposition can cause reduced myocardial contractility and thus can affect the values of strain. Irreversible myocyte damage of the subendocardial fibers, which are usually affected first, can therefore be identified via reduced GLS in the early stages [67]. In addition, altered GCS values can be especially useful for the differentiation between transmural and non-mural cardiac infarction [105]. Moreover, in the presence of inhomogeneous tissue properties, e.g. due to storage or infiltrative disease, myocardial contractility is initially disturbed in the affected regions [67]. For instance, in cardiac amyloidosis impaired longitudinal strain values in the areas of regional hypertrophy are reported [106]. In addition, regional variations of peak systolic strain from apical to basal, also called apical sparing, are described as an accurate screening tool for the differentiation of cardiac amyloidosis and other diseases leading to LV myocardial thickening [107].

It is also important to consider that strain values are mainly influenced by the definition of end-systolic (ES) and ED points in time. It has been established that a change of only 4 frames results in a significant change in strain measurements [108].

1.3.7 Strain Imaging versus Left Ventricular Ejection Fraction

LVEF represents the left ventricular systolic function and is usually assessed via 2D TTE. Hereby, using the biplane Simpson method is recommended [84]. Its unit is a percentage (%).

$$EF = \frac{(EDV - ESV)}{EDV} * 100$$

Figure 10: *Calculation of the ejection fraction.*

The measurement of LVEF is an important factor for the determination of the severity of the reduction of systolic function and thus is useful for the proper management of different CVDs, e.g. heart failure and valvular heart disease [109]. The standard range of LVEF is defined as 52% to 72% for males and 54% to 74% for females [84,109]. The value is mainly influenced by afterload and preload as well as myocardial contraction [110].

However, LVEF and global strain are both parameters reflecting the global function of the left ventricle. While LVEF considers both length and diameter change, GLS only takes one of these components into account [67]. Via mathematical models it has been shown that LVEF can remain unchanged despite significantly decreased LV function. LVEF can be increased due to raised wall thickness and/or reduced end-diastolic volume (EDV) and therefore be within standard range, although myocardial shortening is reduced. In addition, since LVEF is square depending on circumferential shortening, but only linearly depending on length shortening, this parameter is less sensitive to reduced longitudinal shortening [111]. Regarding loading conditions it is also reported that strain is more dependent on preload while LVEF is more dependent on afterload [112].

Compared to LVEF, strain imaging represents a more sensitive diagnostic tool for the detection of discrete systolic dysfunction and the prediction of severe cardiac events [113]. For example, LV dysfunction due to cardiotoxicity after chemotherapeutic treatment initially results in reduced GLS while LVEF is reduced only later [114]. Therefore, GLS is a useful diagnostic tool for patients undergoing chemotherapy to detect cardiotoxicity in the early stages [115,116]. For many other diseases, e.g. primary mitral regurgitation, chronic aortic regurgitation, and asymptomatic diabetes mellitus type 2 GLS is also reported to be a sensitive parameter for minimal changes in myocardial contractility with preserved LVEF [101,103,117,118].

1.3.8 Strain in Arterial Hypertension

In patients with hypertension disease, LVH represents a proven risk factor for the development of asymptomatic LV dysfunction and congestive heart failure [119]. Using conventional echocardiography, asymptomatic diastolic dysfunction associated with LVH can be identified [120]. However, conventional TTE and TDI usually cannot detect discrete changes in LV systolic function due to arterial hypertension in the early stages [121]. Since GLS mainly relates to LV longitudinal function of subendocardial myofibers involved in the early stages of cardiac damages [122], GLS enables a new screening method for early LV risk stratification in patients with hypertension disease [123].

1.4 Gaps in Evidence

The benefits of the polyamine spermidine, a natural autophagy inducer, have been increasingly researched in recent years. Although there is much data on the effects of spermidine based on animal models available, the data on human studies are considerably limited. In a rodent animal study, the cardioprotective benefits of spermidine like lowering blood pressure have already been established [124]. However, experimental data about the cardioprotective effects of dietary spermidine supplementation in hypertensive patients are still restricted. Thus, it is important to determine the impacts of this polyamine on human myocardial function. In addition, although numerous studies have been conducted on the importance and significance of strain imaging in various cardiac diseases, there are still no general

valid recommendations for the interpretation of strain values in patients with arterial hypertension.

1.5 Aims of the Thesis

The main aim of this thesis is to show the functional effects of the treatment with the polyamine spermidine on human myocardial function in patients with hypertension disease and preserved ejection fraction, also known as heart failure with preserved ejection fraction (HFpEF), assessed by echocardiography. For this purpose, certain offline echocardiographic parameters and strain analyses are investigated for the evaluation of LV systolic and diastolic heart function. At the same time, this work aims to evaluate the effects of spermidine on the left atrium and right ventricle.

2 Material and Methods

2.1 Study Design

The Spermidine Anti-Hypertension Study (SMARTEST) is a prospective, single-centered, randomized, double-masked, and placebo-controlled interventional study with crossover assignment. The SMARTEST trial was performed at the Department of Cardiology at the Medical University of Graz. An ethics application (reference number: 30-468 ex 17/18) was granted by the Medical University of Graz for the conduct of the study in advance.

The SMARTEST trial was initiated in February 2020 and is expected to be completed by the end of 2024. According to the trial plan, 46 individuals are planned to participate in this study in total, whereby for this diploma thesis a patient cohort of 20 was analyzed. Patients were treated with 4mg spermidine per day as well as a placebo for a duration of eight weeks each in a crossover design with a four-week washout interval in between.

2.2 Study Population

Inclusion criteria encompassed persistent arterial hypertension with SBP levels of 150 mmHg as a minimum during the hospital stay and the date of randomization. Furthermore, included patients had to receive antihypertensive premedication with at least two first-line recommended blood pressure-lowering drugs according to the 2018 ESC/ESH guidelines [1]. Additionally, the submission of a signed and dated written consent was a mandatory prerequisite. In terms of gender and age, individuals older than 18 years of all genders were eligible.

Exclusion criteria applied in case of SBP ≥ 180mmHg on the date of randomization, spermidine intolerance, renal insufficiency with a glomerular filtration rate of less than 45 ml/min, and insulin-dependent diabetes mellitus. Furthermore, patients with wheat allergy, gluten intolerance, a life expectancy of less than one year, and participation in another clinical study already were excluded.

2.3 Data Collection

2.3.1 Transthoracic Echocardiography

TTE was performed on each patient by expert cardiologists at the Department of Cardiology at the Medical University of Graz at four fixed points in time: 0 weeks (visit 1 *(V1)* = baseline), 8 weeks (visit 2 *(V2)*), 12 weeks (visit 3 *(V3)*), and 20 weeks (visit 4 *(V4)*) after recruitment. The investigations were carried out with the ultrasound device Acuson 2000 by Siemens (Munich, Germany) or Vivid E95 by GE Healthcare (Chalfont St. Giles, UK). For adequate imaging, the frame rate was adjusted between 50 to 70 frames per second. During the examination, three electrodes were attached for an ECG to display the cardiac cycle at the same time.

A TTE contained B-Mode imaging in 2D, 3D, and Doppler image acquisition. In detail, a TTE included parasternal long axis view (PLAX), parasternal short axis view (PSAX) showing the aortic valve, mitral valve, papillary muscles, and apex of the heart, apical two chamber view (A2C), apical three chamber view (A3C), apical four chamber view (A4C), and apical five chamber view (A5C) as well as subcostal four chamber view. In addition, apical views focusing on the left ventricle and left atrium were recorded to provide more precious offline postprocessing measurements if possible. From each of these views, three heart cycles were stored for sinus rhythm and five heart cycles in case of atrial fibrillation. The recorded images and loops were transmitted to the digital archive system IntelliSpace Cardiovascular (ISCV) of the company Philips (Eindhoven, Netherlands) afterwards.

2.3.2 Postprocessing Imaging

For this trial, the entire digital data analysis was performed retrospectively offline. Postprocessing imaging and further offline analyses of selected appropriate 2D trial standard apical view images were carried out with the Software TomTec (TOMTEC Imaging Systems, Munich, Germany). Moreover, the postprocessing speckle tracking software 2D Cardiac Performance Analysis (2D CPA, TOMTEC Imaging Systems, Munich, Germany) was used for triplane calculations and the assessment of the LV GLS, LA GLS, and global average strain. For data analysis, the echocardiographic images stored in ISCV were imported as DICOM files to TomTec

and 2D CPA. All analyses were performed twice, ideally in two consecutive cardiac cycles. In case of very poor image quality of the digitally stored loops, the two most appropriate heart cycles were selected for data analysis. Using the ECG curve, the ES and ED time of the cardiac cycle could be manually determined offline, using the same frame for both. Subsequently, the ES and ED volumes could be measured by manually contouring the ventricle or atrium and adjusting the longitudinal alignment.

2.3.3 Strain Assessment

The assessment of strain was carried out with two different analysis techniques using A2C, A3C, and A4C: AutoStrain and 2D CPA GLS. The following simplified formula was used for the calculation of both methods:

$$GLS = \frac{L_S - L_D}{L_D}$$

Figure 11: *Calculation of the global longitudinal strain.*

2.3.3.1 Left Ventricular AutoStrain

AutoStrain by TOMTEC Imaging Systems (Munich, Germany) is a speckle tracking software that provides an automated triplane strain assessment for LV longitudinal strain along the endocardium.

For the automated strain analysis, manual assignment of the selected apical loops as A4C, A2C, and A3C view was necessary first. Thus, AutoStrain automatically detected the endomyocardial contours, which could be modified manually afterwards. Automated AutoStrain analyses provided color-coded displaying of dynamic longitudinal strain results, ES strain, and time-to-peak strain, each shown as an 18-segment bull's-eye view as well as a table listing the results of the triplane strain analysis.

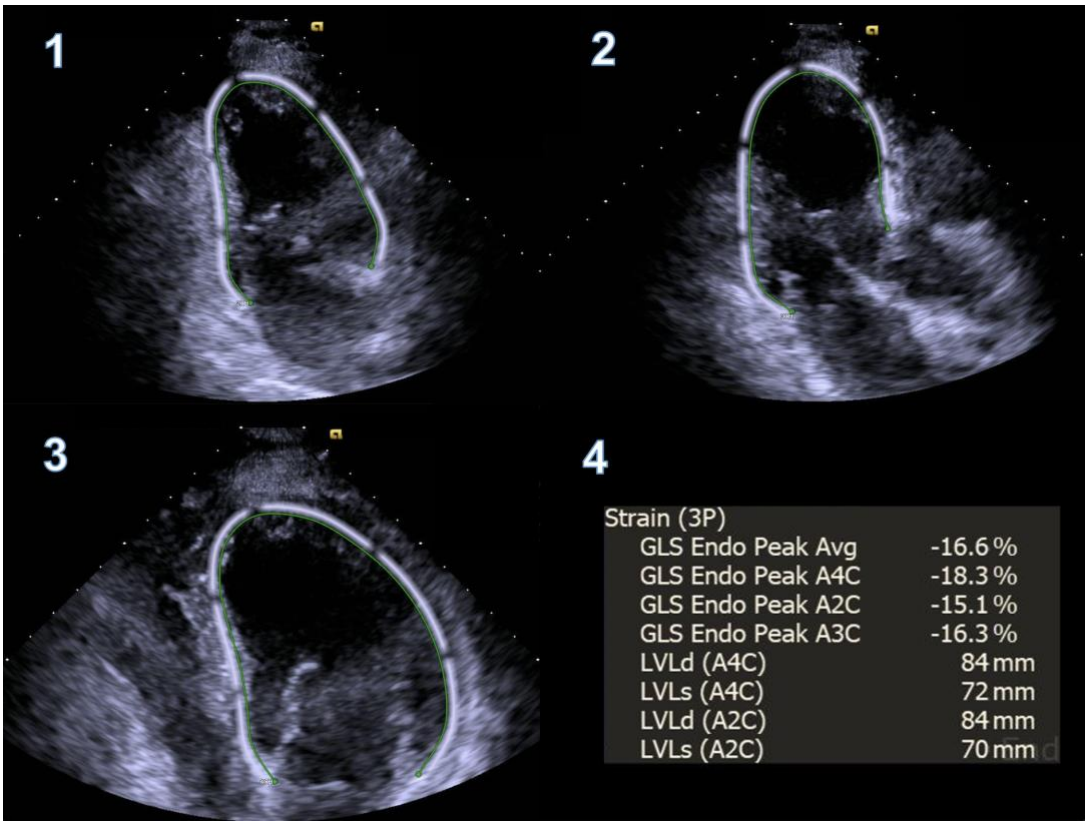

Figure 12: *Example of a strain analysis. Left ventricular global longitudinal strain value of -16.6%. The speckle tracking software AutoStrain by TOMTEC Imaging Systems was used. 1: two chamber view, 2: three chamber view, 3: left ventricular focused four chamber view, 4: results of the strain analysis.*
LVLd = left ventricular length in diastole, LVLs = left ventricular length in systole.

2.3.3.2 2D CPA Global Longitudinal Strain

2D CPA is a 2D speckle tracking software by TOMTEC Imaging Systems (Munich, Germany) and provides a semiautomatic offline analysis of cardiac deformation. For the LV strain assessment with 2D CPA, the selected digitally stored echocardiographic B-mode images had to be assigned manually to A4C, A2C, and A3C first. After that, one heart cycle of the loop and its ES and ED time were defined in M-Mode. Subsequently, the reference points at the mitral annulus and the apex of the left ventricle had to be set in the ES time point for automatic border detection of both endocardial and epicardial contours. For a more precious analysis, the automatically generated contours could be manually readjusted afterwards. After confirmation of the ES ventricle contours, the software automatically created ED border contours.

Strain assessment of the left atrium with 2D CPA was performed largely in the same way, except that for this analysis only an A4C was required, and the LA reference points were defined in ED time, which consisted of the mitral annulus and the roof of the left atrium.

2D CPA strain analysis results included a color rendering of regional myocardial function in-loop, SR curves, 16-segment bull's-eye plots, and a table listing the triplane calculated parameters.

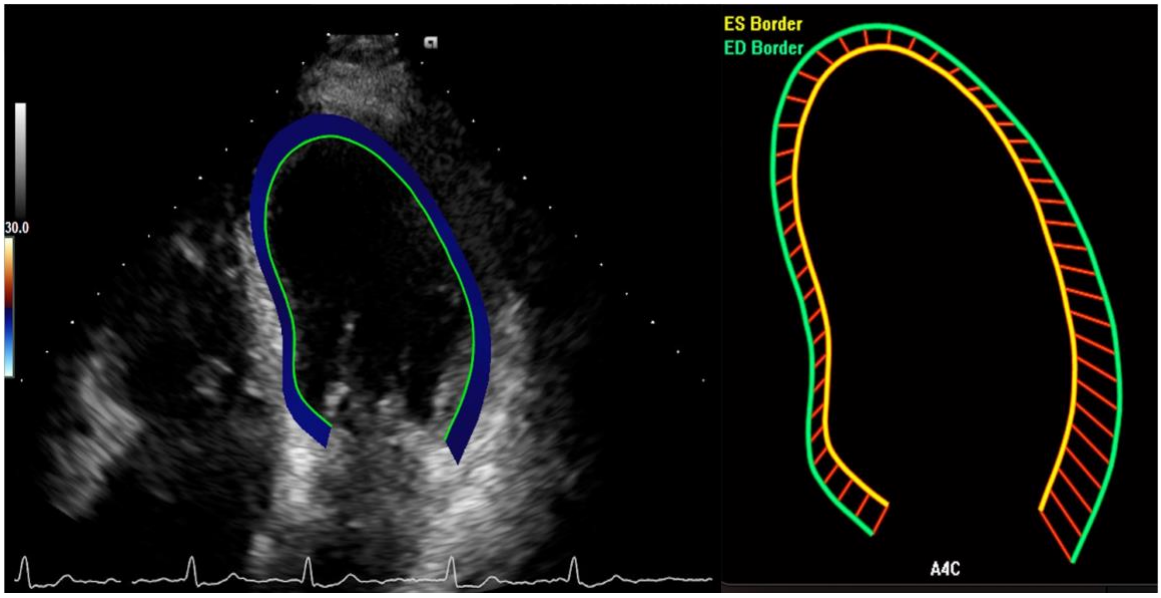

Figure 13: *Example of an endomyocardial contouring of the left ventricle in an apical four chamber view. The speckle tracking software 2D CPA by TOMTEC Imaging Systems was used.*

2.3.4 Calculated Parameters

For this diploma thesis, further parameters describing heart function and heart deformation were measured and calculated, as summarized in Table 4.

LV SV was calculated in both biplane and triplane. According to the Simpson method of SV calculation, the EDV and the end-systolic volume (ESV) were determined for the biplane SV in the A4C and A2C with TomTec. Data collection for triplane calculation of the LV SV was performed with the software 2D CPA using EDV and ESV in A2C, A3C, and A4C.

For the calculation of LV SV following formula was applied, using either biplane or triplane EDV and ESV:

$$SV = EDV - ESV$$

Figure 14: *Calculation of the stroke volume.*

LVEF was also calculated twice in biplane and triplane. According to the Simpson method, the biplane LVEF was determined automatically by TomTec based on the EDV and ESV in A4C and A2C. The triplane LVEF was also calculated automatically by the software 2D CPA using the EDV and ESV of the A4C, A2C, and A3C.

The left ventricular outflow tract (LVOT) SV was determined with the following formula:

$$LVOT\ SV\ = \left(\frac{LVOT}{20}\right)^2 * \pi * VTI_{LVOT}$$

$$\text{VTI} = \text{velocity time integral [cm]}, \text{LVOT} = \text{left ventricular outflow tract [mm]}$$

Figure 15: *Calculation of the left ventricular outflow tract stroke volume.*

Via the following formula, the left atrial volume (LAV) was mathematically calculated:

$$LAV = \frac{8}{3} * \pi * \frac{A_{4CH} * A_{2CH}}{L}$$

$$\text{A} = \text{ left atrial area } [\text{ml/m}^2], \text{L} = \text{left atrial major axis [cm]}$$

Figure 16: *Calculation of the left atrial volume.*

Moreover, linear measurements of the left atrium were performed.

In addition, existing data on the right ventricle and diastolic function were included in this work. For the evaluation of the RV function, the parameters RV basis diameter and tricuspid annular plane systolic excursion (TAPSE) were used. Diastolic function was assessed via the parameters e' lateral, e' septal, E/A ratio, and E/e' ratio.

Table 4: *Executive summary of the measured and calculated parameters.*

Parameter	Unit
LV EDV biplane	ml
LV ESV biplane	ml
LV EDV triplane	ml
LV ESV triplane	ml
LV SV biplane	ml
LV SV triplane	ml
LVOT SV	ml
LV diameter ED	mm
LV septum thickness	mm
LVEF biplane	%
LVEF triplane	%
LV AutoStrain	%
LV GLS	%
LAV	ml
LA GLS	%
RV basal diameter	mm
TAPSE	mm
e' septal	cm/s
e' lateral	cm/s
E/A ratio	*no dimension*
E/e' ratio	*no dimension*

2.4 Statistical Analysis

The required data obtained in TomTec were manually transferred into an Excel sheet (Microsoft Office 365, Microsoft Corporation, Redmond, US). The results of the strain analysis performed with 2D CPA were exported via a created macro into a separate Excel file and checked for plausibility subsequently. After merging both

files, the dataset was further statistically analyzed using the statistical program IBM SPSS Statistics 29 (IBM Corporation, Armonk, New York, US).

All data collected was tested for normal distribution and variance homogeneity. Normal distribution was evaluated both graphically with histograms and Q-Q-plots and mathematically with the Shapiro-Wilk test. The z-standardized values of skewness and kurtosis were additionally calculated and results up to ± 1.96 were interpreted as normally distributed [125]. If not otherwise declared, values are presented as mean ± standard deviation. This is also true for non-normally distributed parameters to promote the readability of the results. In this work, LV volumes, LV diameter ED, LV septum thickness, LVEF, LV strains, LAV, LA GLS *(V1),* RV basal diameter, TAPSE, e' septal, e' lateral, E/A ratio *(V1)*, and E/e' ratio *(V4)* were normally distributed. LA GLS *(V4)*, E/A ratio *(V4),* and E/e' ratio *(V1)* did not meet the criteria of normal distribution. For LA GLS *(V4)* and E/e' ratio *(V1)* normal distribution could be achieved by logarithmizing (log10). Nevertheless, the initial non-normally distributed measurement values are given in the text for better comparability.

Furthermore, the absolute differences in LV volumes, LV diameter ED, LV septum thickness, LVEF, LV strains, LAV, LA GLS, RV diameter basis, TAPSE, e' septal, e' lateral, E/A ratio, and E/e' ratio between visit 1 and visit 4 (V4-V1) were determined and the paired t-test was used to analyze the significance of these metric parameters. Although the absolute differences in LAV showed a z-standardized skewness and in LA GLS and RV diameter a z-standardized kurtosis value slightly above + 1.96, they were also assumed to be normally distributed due to their graphical representation and results of the Shapiro-Wilk tests. For correlation analysis of echocardiographic parameters at visit 4, Spearman's rank-order correlation was performed. For all tests, results with (two-sided) p-values < 0.05 were considered statistically significant.

For a clear presentation of the results, tables (Microsoft Word 365, Microsoft Excel 365) and box plots (IBM SPSS Statistics 29) were created.

3 Results

For a better overview, the results of descriptive statistics and correlation analysis are summarized in Tables 5 and 6.

3.1 Subjects

In total, 20 subjects were included in this data analysis. Regarding gender distribution, 60% (n = 12) were males and 40% (n = 8) were females. The age of the patients ranged between 49 and 79 years with an average age of 66.69 ± 8.80 years (female 67.68 ± 9.52 years, male 66.03 ± 8.66 years). The youngest and the oldest study participants were both male.

3.2 Left Ventricular Volumes

Baseline *(V1)* biplane LV EDV, LV ESV, and LV SV were assessed in 18 subjects (10 in the male group, 8 in the female group). Mean biplane LV EDV (*V1)* was 133.73 ± 27.88 ml (males 147.83 ± 24.51 ml, females 116.11 ± 21.82 ml), the mean biplane LV ESV *(V1)* was 69.01 ± 20.72 ml (males 77.38 ± 17.62 ml, females 58.55 ± 20.46 ml) and the mean biplane LV SV *(V1)* was 64.72 ± 18.72 ml (males 70.45 ± 20.23 ml, females 57.56 ± 14.83 ml).

On visit 4/4 biplane LV EDV, LV ESV, and LV SV were evaluated in 16 subjects (9 in the male group, 7 in the female group). The average biplane LV EDV *(V4)* was 135.22 ± 19.08 ml (males 151.51 ± 28.90 ml, females 114.25 ± 19.38 ml), the average biplane LV ESV *(V4)* was 71.82 ± 19.08 ml (males 82.38 ± 12.71 ml, females 58.25 ± 17.67 ml) and the average biplane LV SV *(V4)* was 63.40 ± 19.43 ml (males 69.16 ± 22.68 ml, females 56.00 ± 12.02 ml).

The null hypothesis, that there are no significant differences in biplane LV EDV, LV ESV, and LV SV between visit 1 and visit 4, could not be rejected with p-values of 0.722 (biplane LV EDV), 0.961 (biplane LV ESV), and 0.788 (biplane LV SV).

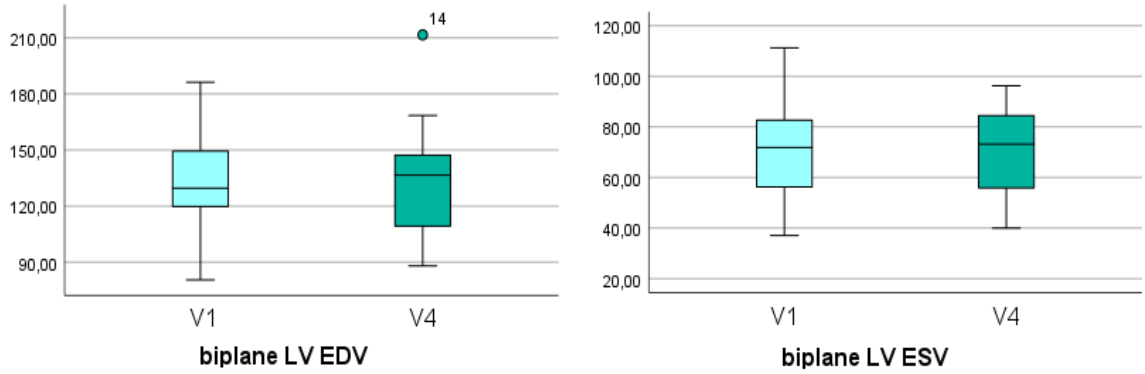

Figure 17: *Boxplots of biplane LV EDV and biplane LV ESV at visit 1 and visit 4. No significant differences between visit 1 and visit 4.*

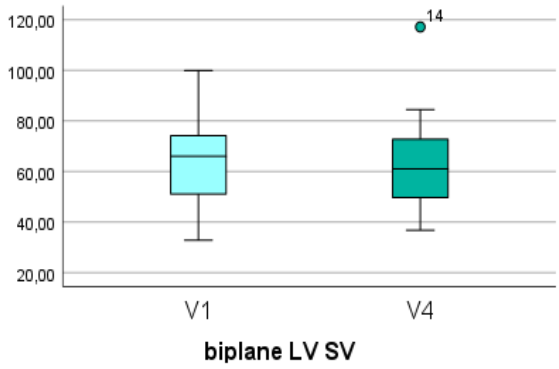

Figure 18: *Boxplot of biplane LV SV at visit 1 and visit 4. No significant difference between visit 1 and visit 4.*

Baseline *(V1)* triplane LV EDV, LV ESV, and LV SV were also available in 18 patients (10 in the male group, 8 in the female group) and were comparable with the mean biplane volume measurements: The mean triplane LV EDV *(V1)* was 134.63 ± 30.93 ml (males 148.45 ± 29.91 ml, females 117.36 ± 21.81 ml), the mean triplane LV ESV *(V1)* was 67.85 ± 19.02 ml (males 74.92 ± 17.42 ml, females 59.02 ± 18.11 ml), and the mean triplane LV SV *(V1)* was 66.78 ± 21.16 ml (males 73.54 ± 23.66 ml, females 58.34 ± 14.87 ml).

Visit 4/4 triplane LV volume measurements (LV EDV, LV ESV, LV SV) were assessed in only 13 patients (9 in the male group, 4 in the female group). Nevertheless, mean triplane volumes were comparable to mean biplane volumes: The mean triplane LV EDV *(V4)* was 138.68 ± 31.66 ml (males 148.72 ml ± 29.55 ml, females 116.09 ± 26.42 ml), the mean triplane LV ESV *(V4)* was 71.90 ± 15.90 ml (males 76.45 ± 13.06 ml, females 61.66 ± 18.84 ml), and the mean triplane LV SV *(V4)* was 66.78 ± 21.05 ml (males 72.27 ± 20.20 ml, females 54.4 ± 19.79 ml).

There were no significant differences in triplane LV EDV, LV ESV, and LV SV between visit 1 and visit 4 with p-values of 0.898 (triplane LV EDV), 0.676 (triplane LV ESV), and 0.473 (triplane LV SV).

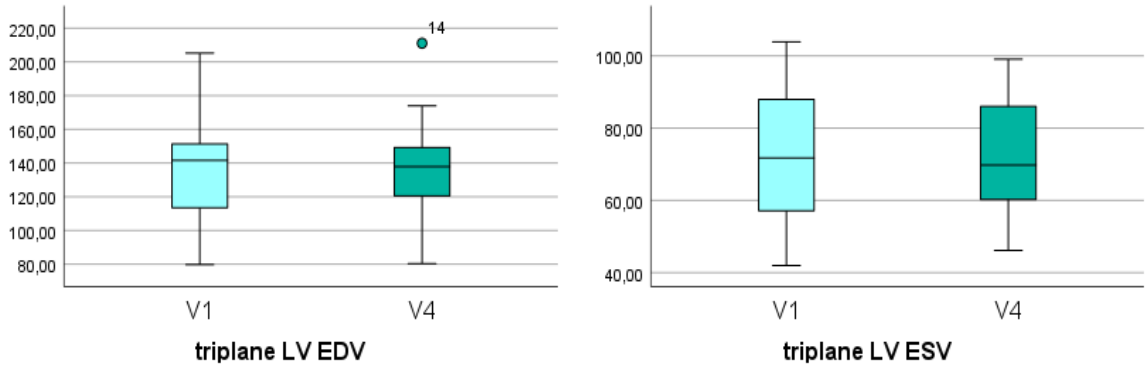

Figure 19: *Boxplots of triplane LV EDV and triplane LV ESV at visit 1 and visit 4. No significant differences between visit 1 and visit 4.*

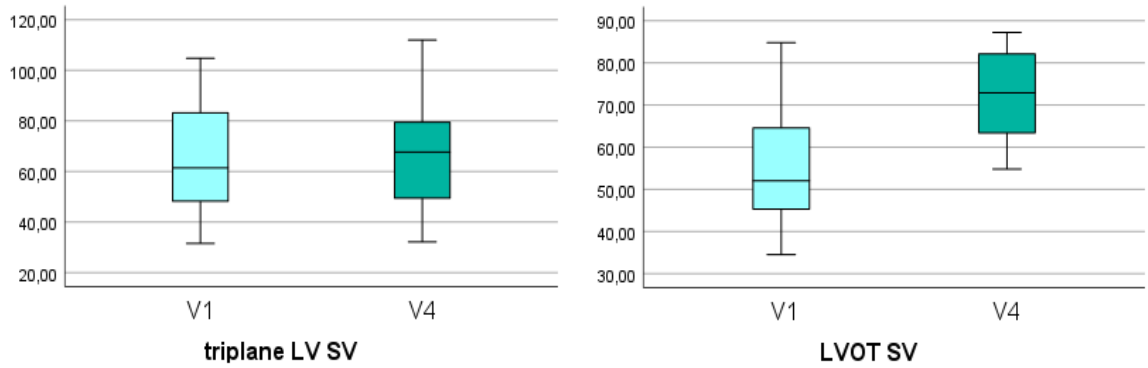

Figure 20: *Boxplots of triplane LV SV and LVOT SV at visit 1 and visit 4. Triplane LV SV: No significant difference between visit 1 and visit 4. LVOT SV: Significant difference between visit 1 and visit 4.*

LVOT SV *(V1)* was available in 13 subjects (6 in the male group, 7 in the female group). The average value was 61.61 ± 15.43 ml, higher in males with 67.97 ± 5.77 ml than in females with 56.16 ± 19.32 ml. On visit 4/4 LVOT SV was only assessed in 9 patients (4 in the male group, 5 in the female group) and the mean value was 73.41 ± 10.99 ml, again with gender-specific differences (males 79.75 ± 3.26 ml, females 68.34 ± 12.70 ml). Although the paired t-test showed a significant difference in the LVOT SV values between visit 1 and visit 4 with a p-value of 0.024, absolute LVOT SV did only change by 16.41 ± 14.45 ml in individuals who underwent visit 1 and visit 4.

3.3 Left Ventricular Diameter End-Diastolic and Left Ventricular Septum Thickness

Baseline *(V1)* LV diameter ED and LV septum thickness were evaluated in 13 patients (5 in the male group, 8 in the female group). The mean value of LV diameter ED *(V1)* was 49.31 ± 6.10 mm, higher in men compared to women (males 51.80 ± 7.36 mm, females 47.75 ± 5.06 mm). The average value of LV septum thickness *(V1)* was 11.62 ± 2.72 mm, higher in women than in men (males 10.40 ± 0.89 mm, females 12.37 ± 3.25 mm).

On visit 4/4 LV diameter ED and LV septum thickness were only assessed in 10 subjects (4 in the male group, 6 in the female group). The average value of LV diameter ED *(V4)* was 52.5 ± 5.52 mm, again higher in men than women (males 55.50 ± 6.76 mm, females 50.50 ± 3.94 mm). The mean value of LV septum thickness *(V4)* was 11.90 ± 1.97 mm, also higher in women compared to men (males 11.25 ± 1.71 mm, females 12.33 ± 2.16 mm).

The null hypothesis, that there are no significant differences in both LV diameter ED and LV septum thickness between visit 1 and visit 4, could not be rejected with p-values of 0.214 (LV diameter ED) and 0.604 (LV septum thickness).

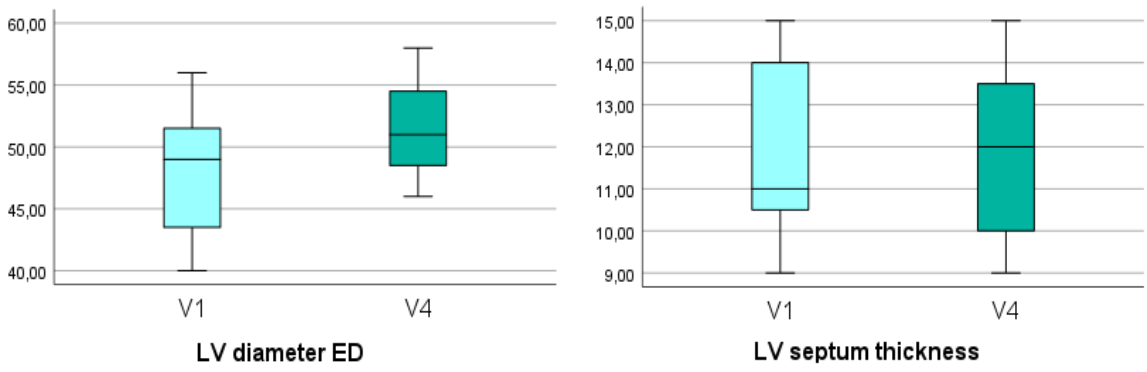

Figure 21: *Boxplots of LV diameter ED and LV septum thickness at visit 1 and visit 4. No significant differences between visit 1 and visit 4.*

3.4 Left Ventricular Ejection Fraction

On V1/4 both biplane and triplane LVEF were assessed in 18 patients (10 in the male group, 8 in the female group) and the average values were comparable with one another: The mean biplane LVEF *(V1)* was 49 ± 10.6% (males 47 ± 10.0%, females 50 ± 11.9%) and the mean triplane LVEF *(V1)* was 50 ± 9.8% (males 49 ± 9.3%, females 50 ± 11.0%). Biplane LVEF *(V1)* values were < 40% in 11.11% (n = 2), between 40 - 49% in 38.89% (n = 7), and ≥ 50% in 50.00% (n = 9). Triplane LVEF measurement results were < 40% in 16.67% (n = 3), between 40 - 49% in 38.89% (n = 7), and ≥ 50% in 44.44% (n = 8).

On V4/4 biplane LVEF was evaluated in 16 subjects (9 in the male group, 7 in the female group). The average biplane LVEF *(V4)* was 47 ± 8.7% (males 45 ± 7.5%, females 50 ± 10.0%). Through biplane evaluation, LVEF *(V4)* was < 49% in 18.75% (n = 3), between 40 - 49% in 31.25% (n = 5), and ≥ 50% in 50.00% (n = 8) of all patients. Triplane LVEF *(V4)* was only available in 13 subjects (9 in the male group, 4 in the female group). The average triplane LVEF *(V4)* value was 48 ± 7.4% (males 48 ± 5.8% and females 47 ± 11.4%) and therefore comparable with biplane measurement results. Triplane LVEF (V4) values were < 40% in 15.38% (n = 2), between 40 - 49% in 30.77% (n = 4), and ≥ 50% in 53.85% (n = 7).

The null hypothesis, that there are no significant differences in biplane and triplane LVEF between visit 1 and visit 4, could not be rejected with p-values of 0.906 (biplane LVEF) and 0.554 (triplane LVEF).

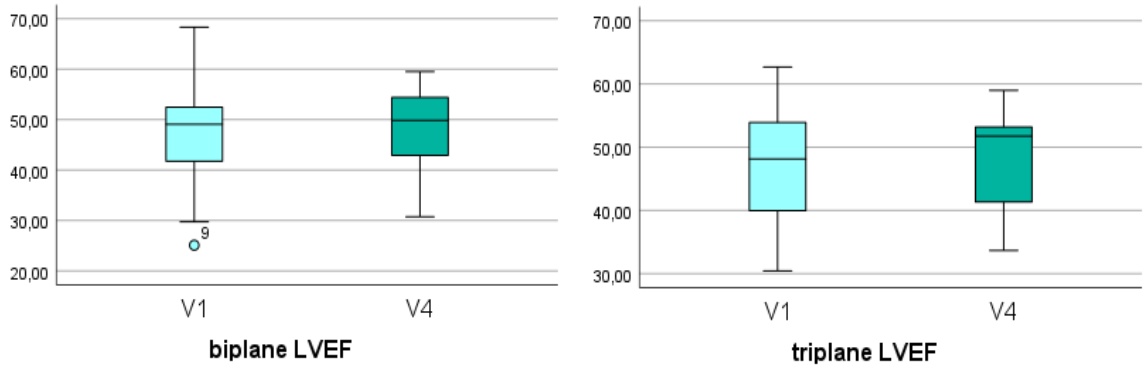

Figure 22: *Boxplots of biplane and triplane LVEF at visit 1 and visit 4. No significant differences between visit 1 and visit 4.*

3.5 Left Ventricular AutoStrain and Left Ventricular Global Longitudinal Strain

Baseline LV AutoStrain *(V1)* was evaluated in 17 patients (10 in the male group, 7 in the female group). The average LV AutoStrain was -19.39 ± 3.63%, quite similar for both genders (males -19.55 ± 3.31%, females -19.17 ± 4.31%). LV AutoStrain *(V4)* was available in 13 patients (8 in the male group, 5 in the female group) with a mean value of -18.13 ± 3.37%. The average LV AutoStrain *(V4)* was lower in males compared to females (males -17.54 ± 2.33%, females -19.09 ± 4.77%). The null hypothesis, that there is no significant difference in LV AutoStrain between visit 1 and visit 4, could not be rejected with a p-value of 0.460.

LV GLS *(V1)* was assessed in 18 subjects (10 in the male group, 8 in the female group). The mean LV GLS was -18.19 ± 3.86% without significant gender-dependent differences (males -18.17 ± 4.24%, females -18.22 ± 3.61%). On visit 4/4 LV GLS was only available in 13 patients (9 in the male group, 4 in the female group). The mean LV GLS *(V4)* value was -17.36 ± 3.78%, slightly higher in males with -17.95 ± 3.47% than in females with -16.05 ± 4.67%. There was no significant difference in LV GLS between visit 1 and visit 4 with a p-value of 0.748.

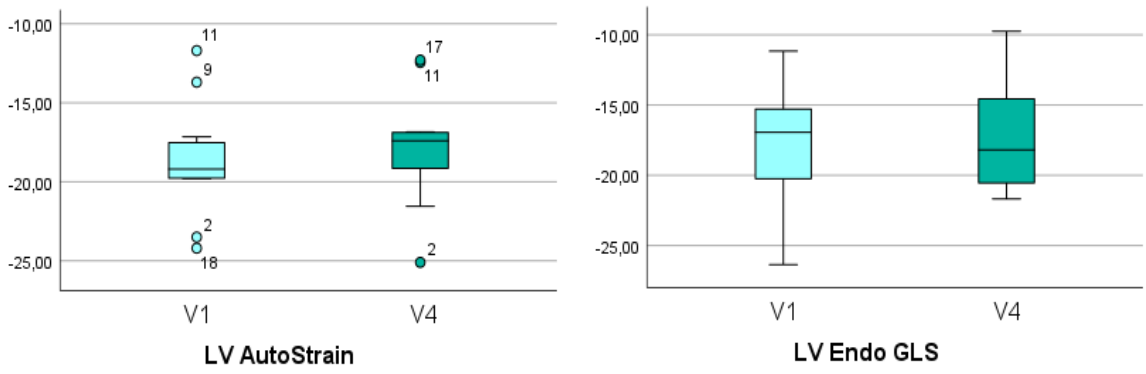

Figure 23: *Boxplots of LV AutoStrain and LV Endo GLS at visit 1 and visit 4. No significant differences between visit 1 and visit 4.*

3.6 Left Atrial Volume and Left Atrial Global Longitudinal Strain

LAV (V1) was available in 18 subjects (10 in the male group, 8 in the female group). The mean LAV (V1) was 69.86 ± 21.20 ml without significant differences between both gender groups (males 70.07 ± 18.87 ml, females 69.57 ± 25.16 ml). On visit 4/4 LAV was assessed in 16 patients (9 in the male group, 7 in the female group) and the average value was 67.15 ± 21.47 ml, also quite similar for men and women (males 66.70 ± 19.51 ml, females 67.73 ± 25.37 ml). There was no significant difference in LAV between visit 1 and visit 4 with a p-value of 0.676.

Baseline LA GLS *(V1)* was evaluated in 18 subjects (10 in the male group, 8 in the female group). The average value was 27.91 ± 11.35%, whereby men had higher values compared to women (males 29.70 ± 9.03%, females 25.66 ± 14.05%). LA GLS *(V4)* was assessed in 15 patients (9 in the male group, 6 in the female group) and the average value was 27.65 ± 17.22%, slightly higher in men with 28.05 ± 10.77% than in women with 27.06 ± 25.37%. The null hypothesis, that there is no significant difference in LA GLS between visit 1 and visit 4, had to be retained with a p-value of 0.897.

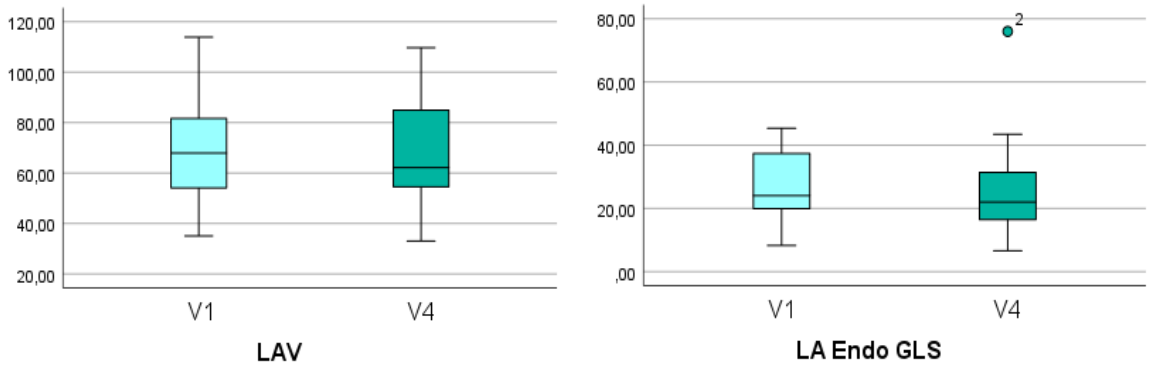

Figure 24: *Boxplots of LAV and LA Endo GLS at visit 1 and visit 4. No significant differences between visit 1 and visit 4.*

3.7 Right Ventricular Basal Diameter and Tricuspid Annular Plane Systolic Excursion

RV basal diameter *(V1)* was assessed in 15 patients (8 in the male group, 7 in the female group). The average RV basal diameter *(V1)* was 31.67 ± 7.52 mm with similar values for both genders (males 32.00 ± 8.45 mm, females 31.29 ± 6.95 mm). On visit 4/4 RV basal diameter was available in only 11 subjects (6 in the male group, 5 in the female group) with a mean value of 35.54 ± 5.28 mm, almost the same for women and men (males 35.50 ± 5.68 mm, females 35.60 ± 5.41 mm). The paired t-test showed no significant difference in RV basal diameter between visit 1 and visit 4 with a p-value of 0.214.

Tricuspid annular plane systolic excursion (TAPSE) *(V1)* was evaluated in 13 patients (7 in the male group, 6 in the female group). The average TAPSE *(V1)* was 23.00 ± 3.58 mm, slightly higher in men than in women (males 23.86 ± 3.24 mm, females 22.00 ± 4.00 mm). TAPSE *(V4)* was assessed in 11 patients (6 in the male group, 5 in the female group). The mean TAPSE *(V4)* was 22.18 ± 2.64 mm without significant gender-specific differences (males 22.33 ± 3.20 mm, females 22.00 ± 2.12 mm). The null hypothesis, that there is no significant difference in TAPSE between visit 1 and visit 4, could not be rejected with a p-value of 0.229.

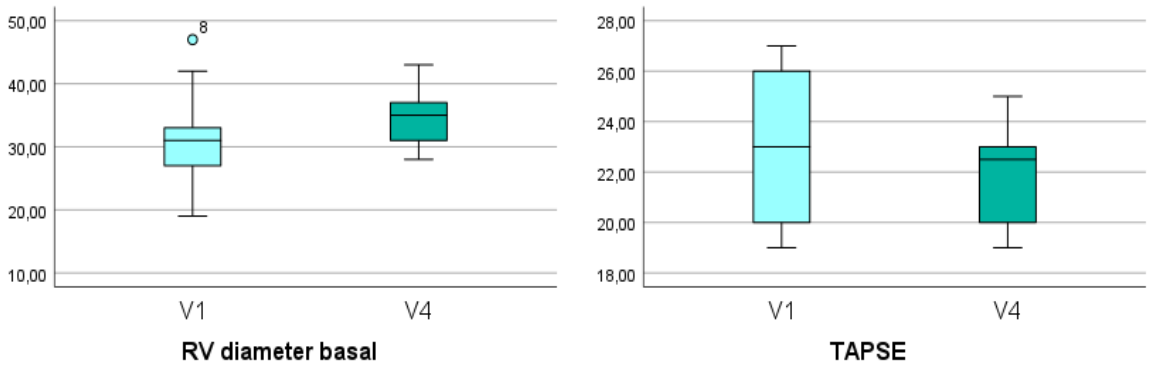

Figure 25: *Boxplots of RV diameter basal and TAPSE at visit 1 and visit 4. No significant differences between visit 1 and visit 4.*

3.8 E’ Septal, E’ Lateral, E/A Ratio and E/e’ Ratio

E‘ septal *(V1)* was available in 13 patients (7 in the male group, 6 in the female group). The mean e’ septal was 6.41 ± 1.51 cm/s, slightly higher in men than in women (males 6.99 ± 1.65 cm/s, females 5.75 ± 1.11 cm/s). On visit 4/4 e’ septal was only assessed in 8 patients (5 in the male group, 3 in the female group). The average value of e’ septal *(V4)* was 6.36 ± 1.39 cm/s, nearly the same for men as women (males 6.28 ± 1.42 cm/s, females 6.5 ± 1.64 cm/s). There was no significant difference in e’ septal between visit 1 and visit 4 with a p-value of 0.941.

E’ lateral *(V1)* was evaluated in 13 subjects (7 in the male group, 6 in the female group) with a mean value of 8.74 ± 2.00 cm/s, which was slightly higher in women than in men (males 8.40 ± 2.18 cm/s, females 9.13 ± 1.87 cm/s). E’ lateral *(V4)* was available in 10 patients (each 5 in the male and the female group) with an average value of 9.40 ± 1.91 cm/s, also slightly higher in women compared to men (males 8.66 ± 1.93 cm/s, females 10.14 ± 1.76 cm/s). The null hypothesis, that there is no significant difference in e’ lateral between visit 1 and visit 4, had to be retained with a p-value of 0.134.

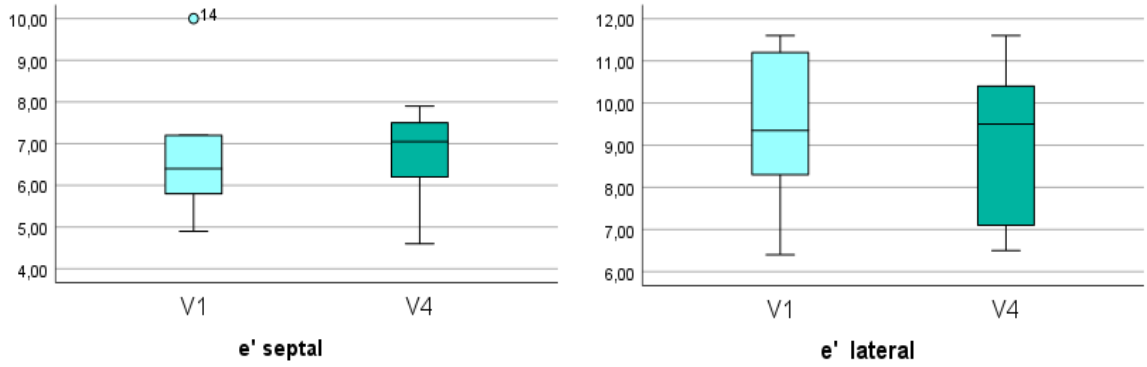

Figure 26: *Boxplots of e' septal and e' lateral at visit 1 and visit 4. No significant differences between visit 1 and visit 4.*

E/A ratio *(V1)* was assessed in 14 patients (8 in the male group, 6 in the female group). The mean E/A ratio *(V1)* was 0.78 ± 0.15 (males 0.79 ± 0.15, females 0.77 ± 0.16). On visit 4/4 the E/A ratio was available in 10 patients (each 5 in the male and female group) with an average value of 1.11 ± 0.58. The E/A ratio *(V4)* was higher in female than in male subjects (males 0.83 ± 0.06, females 1.39 ± 0.75).

The null hypothesis, that there is no significant difference in E/A ratio between visit 1 and visit 4, could not be rejected with a p-value of 0.198.

E/e' ratio *(V1)* was available in 13 patients (6 in the male group, 7 in the female group). The average value was 8.10 ± 1.63, slightly higher in men than in women (males 8.87 ± 0.76, females 7.44 ± 0.43). On visit 4/4 the E/e' ratio was only evaluated in 9 patients (3 in the male groups, 6 in the female group) with a mean value of 8.27 ± 2.15, again slightly higher in men compared to women (males 9.60 ± 2.33, women 7.61 ± 1.91). There was no significant difference in E/e' ratio between visit 1 and visit 4 with a p-value of 0.483.

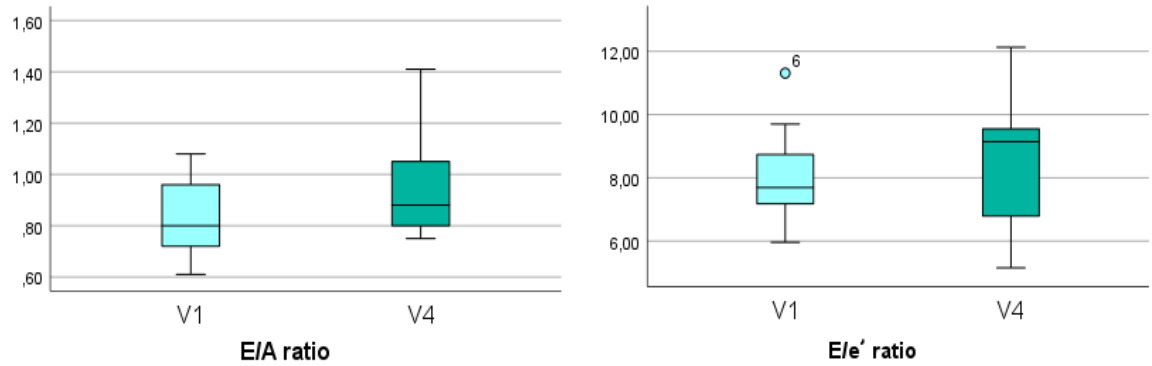

Figure 27: *Boxplots of E/A ratio and E/e' ratio at visit 1 and visit 4. No significant differences between visit 1 and visit 4.*

Table 5: *Descriptive statistics. Values are given as mean ± standard derivation.*

Parameter	Visit	mean ± σ	N
biplane LV EDV	V1	133.73 ± 27.88 ml	18
	V4	135.22 ± 19.08 ml	16
biplane LV ESV	V1	69.01 ± 20.72 ml	18
	V4	71.82 ± 19.08 ml	16
biplane LV SV	V1	64.72 ± 18.72 ml	18
	V4	63.40 ± 19.43 ml	16
triplane LV EDV	V1	134.63 ± 30.93 ml	18
	V4	138.68 ± 31.66 ml	13
triplane LV ESV	V1	67.85 ± 19.02 ml	18
	V4	71.90 ± 15.90 ml	13
triplane LV SV	V1	66.78 ± 21.16 ml	18
	V4	66.78 ± 21.05 ml	13
LVOT SV	V1	61.61 ± 15.43 ml	13
	V4	73.41 ± 10.99 ml	9
LV diameter ED	V1	49.31 ± 6.10 mm	13
	V4	52.5 ± 5.52 mm	10
LV septum thickness	V1	11.62 ± 2.72 mm	13
	V4	11.90 ± 1.97 mm	10
biplane LVEF	V1	49 ± 10.6%	18
	V4	47 ± 8.7%	16
triplane LVEF	V1	50 ± 9.8%	18
	V4	48 ± 7.4%	13
LV AutoStrain	V1	-19.39 ± 3.63%	17
	V4	-18.13 ± 3.37%	13
LV GLS	V1	-18.19 ± 3.86%	18
	V4	-17.36 ± 3.78%	13
LAV	V1	69.86 ± 21.20 ml	18
	V4	67.15 ± 21.47 ml	16
LA GLS	V1	27.91 ± 11.35%	18
	V4	27.65 ± 17.22%	15

Parameter	Visit	mean ± σ	N
RV basis diameter	V1	31.67 ± 7.52 mm	15
	V4	35.54 ± 5.28 mm	11
TAPSE	V1	23.00 ± 3.58 mm	13
	V4	22.18 ± 2.64 mm	11
e' septal	V1	6.41 ± 1.51 cm/s	13
	V4	6.36 ± 1.39 cm/s	8
e' lateral	V1	8.74 ± 2.00 cm/s	13
	V4	9.40 ± 1.91 cm/s	10
E/A ratio	V1	0.78 ± 0.15	14
	V4	1.11 ± 0.58	10
E/e' ratio	V1	8.10 ± 1.63	13
	V4	8.27 ± 2.15	9

3.9 Correlation Analysis

The classification by Cohen [126] of weak ($0.10 \leq r < 0.30$), moderate ($0.30 \leq r < 0.50$), and strong effects ($r \geq 0.50$) was used to interpret the strength of correlation. R-values < 0.10 are trivial [126]. For better illustration, the results are displayed as a correlation matrix (see Table 6).

A strong correlation was shown between biplane SV and biplane LVEF (r = 0.556) as well as LVOT SV and LV diameter ED (r = 0.580). Furthermore, LV Endo GLS and biplane SV (r = -0.516), LVOT SV (r = -0.536), LV septum thickness (r = 0.794) biplane LVEF (r = -0.593), LV AutoStrain (r = 0.651), LA Endo GLS (r = -0.681) as well as RV basis diameter (r = 0.717) correlated strongly. In addition, LV AutoStrain showed a strong correlation with biplane LVEF (r = -0.536), LA Endo GLS (r = -0.666) and LV diameter ED (r = 0.518). Furthermore, LV septum thickness correlated strongly with LA Endo GLS (r = -0.542). Between RV basis diameter and both LAV (r = 0.501) and LV septum thickness (r = 0.731) a strong correlation could also be determined. Moreover, the TAPSE parameter correlated strongly with LVOT SV (r = 0.511), LAV (r = -0.509), and E/A ratio (r = -0.633). E/A ratio further showed a strong effect with LVOT SV (r = -0.669) and LV diameter ED (r = -0.794). In the correlation matrix, the statistically significant ($p < 0.05$) results are marked with the symbol *.

Table 6: *Correlation matrix of volume, linear, and strain parameters at visit 4.*

	biplane SV	LVOT SV	LV diameter ED	LV septum thickness	biplane LVEF	LV AutoStrain	LV Endo GLS	LAV	LA Endo GLS	RV basis diameter	TAPSE	E/A ratio
biplane SV		0.467	-0.167	-0.363	0.556*	-0.047	-0.516	0.191	0.164	-0.282	0.028	-0.438
LVOT SV	0.467		0.580	0.029	0.450	-0.333	-0.536	0.150	0.119	-0.176	0.511	-0.669
LV diameter ED	-0.167	0.580		0.258	0.100	0.518	0.377	0.452	-0.491	0.250	0.165	-0.794
LV septum thickness	-0.363	0.029	0.258		0.051	-0.092	0.794	0.338	-0.542	0.731	0.056	-0.403
biplane LVEF	0.556*	0.450	0.100	0.051		-0.536	-0.593*	0.300	0.239	-0.319	0.009	-0.158
LV AutoStrain	-0.047	-0.333	0.518	-0.092	-0.536		0.651*	0.179	-0.666*	0.318	-0.474	0.108
LV Endo GLS	-0.516	-0.536	0.377	0.794	-0.593*	0.651*		0.247	-0.681*	0.717*	-0.187	0.262
LAV	0.191	0.150	0.452	0.338	0.300	0.179	0.247		-0.375	0.501	-0.509	0.195
LA Endo GLS	0.164	0.119	-0.491	-0.542	0.239	-0.666*	-0.681*	-0.375		-0.365	0.369	-0.276
RV basis diameter	-0.282	-0.176	0.250	0.731	-0.319	0.318	0.717*	0.501	-0.365		-0.105	0.070
TAPSE	0.028	0.511	0.165	0.056	0.009	-0.474	-0.187	-0.509	0.369	-0.105		-0.633
E/A ratio	-0.438	-0.669	-0.794	-0.403	-0.158	0.108	0.262	0.195	-0.276	0.070	-0.633	

● strong correlation ● moderate correlation ● weak correlation ● trivial effect

4 Discussion

In this thesis, echocardiographic changes following spermidine administration in hypertensive individuals showed that 1) there was no change in LV volumes and function, 2) there was no change in RV diameter and function, 3) there was no change in LA diameter and function, and 4) there was no change in parameters reflecting the diastolic function.

4.1 The Role of Transthoracic Echocardiography in Arterial Hypertension

2D TTE has long been proven as a reliable, non-invasive diagnostic tool for the assessment of LV mass [127-129]. It shows higher sensitivity and specificity for the detection of arterial hypertension by identifying LVH compared to ECG [30]. LVH is caused by hypertension-induced persistent pressure overload [30] and has already long been known as a high-risk factor for cardiovascular morbid events and all-cause mortality, independent of age, blood pressure level, and other cardiovascular risk factors [130-132].

In an early report of the Framingham Heart Study already published in 1989, Levy et al. [133] focused on the correlation of LV mass and incidence of coronary heart disease in 406 male and 735 female subjects older than 40 years. This report demonstrated a clear correlation between LVH and the incidence of coronary heart disease for both genders over a follow-up interval of four years. Furthermore, Levi et al. [134] determined that LVH has a negative prognostic effect in middle-aged patients too.

Another very early report published by Casale et al. [135] discussed a higher risk for cardiovascular events in men with mild hypertension disease but pre-existing echocardiographically determined LVH. In this study, 140 male subjects were included of whom 14 showed cardiovascular events in the course.

Verdecchia et al. [131] observed a patient cohort of 2363 initially untreated patients with essential hypertension over 14 years and established a higher risk for stroke and transient ischemic attack in hypertensive patients with diagnosed LVH.

Moreover, Devereux et al. [136] demonstrated in a prospective study including 941 patients with essential hypertension that a reduction in LV mass during antihypertensive therapy results in a lower risk for cardiovascular morbid events.

Similar results are discussed in an extensive published meta-analysis, which included 1064 hypertensive patients. This data also showed an association between the regression of LVH during antihypertensive treatment and a significant decrease in CVD compared to new or enhanced LVH [137].

These published data clarify the importance of 2D TTE for the assessment of LVH and cardiovascular risk evaluation in patients with hypertensive disease. Therefore, TTE has long been established as a significant prognostic tool in the clinical practice of arterial hypertension.

In addition, 2D TTE can be used to assess LV systolic function via LVEF. Given the fact that LVEF can be normal in the case of LV concentric hypertrophy, LVEF does not represent a precise diagnostic value for arterial hypertension [138,139].

In this study, the LV septum thickness was used for the evaluation of LVH. The results of this study showed a mean LV septum thickness of 11.25 ± 1.71 mm for males and 12.33 ± 2.16 mm for females on visit 4. Compared to the normal reference values for each gender (males 6 – 10 mm, females 6 – 9 mm) [84], men and women showed a mild increase in LV septum thickness. Since these patients are suffering from persistent arterial hypertension, even a higher increase in LV septum thickness was to be expected. Based on the published data it can be assumed that these subjects are at higher risk for cardiovascular morbid events.

4.1.1 Diastolic Dysfunction in Arterial Hypertension

Arterial hypertension represents the most common cause of diastolic heart failure [140]. Hypertension-induced LV remodeling affects the LV diastolic function by changes in LV filling rate and LV relaxation [141] and in most hypertensive patients, diastolic LV dysfunction is the first recognizable manifestation of heart disease [142]. Data published a long time ago already reported a reduction of LV filling rate in the early stages of hypertension disease without affected cardiac output or LVEF [141,143]. LV diastolic dysfunction is especially associated with HFpEF [144,145].

TTE is the most used diagnostic tool for the detection of LV diastolic function [146] and should be part of routine diagnostic, especially in subjects with dyspnea or heart failure [147]. There are several echocardiographic parameters to assess LV diastolic function, e.g. e', E/A ratio, E/E ratio, and LA strain [146]. Schillaci et al. [148] observed 1839 hypertensive subjects without prior cardiovascular events up to 11 years. It is reported that an early determination of impaired diastolic relaxation by Doppler techniques enables the detection of hypertensive patients at higher risk for cardiovascular events, independent of LVH and blood pressure levels.

In this work, LV diastolic function was evaluated based on e' lateral, e' septal, E/A ratio, and E/e' ratio. The results of this study showed only slightly reduced LV diastolic function without significant changes between visit 1 and visit 4. A more limited diastolic function was to be expected due to arterial hypertension.

4.2 Deformation Imaging in Arterial Hypertension

Strain analysis represents a relatively new diagnostic tool for the assessment of heart function in patients with cardiac diseases. Even though there is limited evidence regarding the assessment of strain in hypertensive patients, GLS appears to be a reliable parameter for the detection of LV dysfunction [67,84,88,139]. Especially in the early stages of arterial hypertension, deformation imaging seems to be very useful for the detection of systolic dysfunction. Previously published studies reported significantly reduced GLS values in patients with arterial hypertension and preserved LVEF [121,149-151].

Imbalzano et al. [121] looked at the benefits of deformation imaging for the detection of hypertension-induced early subclinical dysfunction and found reduced GLS values in both patients with and without LVH. In contrast, conventional TTE did not detect systolic dysfunction in both groups and TDI did only in the patients with pre-existing LVH.

Gonçalves et al. [149] published a study including hypertensive (n = 229) and normotensive (n = 20) subjects to detect subclinical LV dysfunction in hypertensive patients with preserved LVEF (> 55%) by the assessment of strain. This study

determined subclinical LV dysfunction in 15.3% of all hypertensive patients with the absence of LVEF reduction.

Furthermore, Kosmala et al. [150] compared speckle tracking and TDI strain measurements in hypertensive subjects with heart failure and showed that LV GLS decreased progressively with hypertension-induced heart failure classified by the New York Heart Association (NYHA) I to IV. The comparability of strain values measured by STE and TDI were within acceptable ranges. Changes in LV GCS and GRS were described in the advanced stages of NYHA III and NYHA IV.

Moreover, a small study by Sengupta et al. [151] showed significantly reduced subendocardial and subepicardial longitudinal strain values in hypertensive subjects with preserved LVEF. In contrast, the circumferential strain was only reduced in subepicardial layers, and the radial strain showed no significant reduction in any of the regions.

All in all, GLS appears to be a meaningful parameter for the detection of subclinical LV systolic dysfunction, despite the presence of LVH and reduced LVEF. Therefore, strain analysis could be very useful for adequate clinical management and the assessment of risk for heart failure in hypertensive patients. However, recommendations for international standardized values of strain values in healthy patients and reference values for the interpretation of heart dysfunction in hypertensive patients are still missing.

In this work, for the evaluation of LV heart function strain analyses included LV Endo GLS and LV AutoStrain. As expected, the results of this thesis showed a significantly negative correlation between LV Endo GLS and biplane LVEF ($r = -0.593$) and a significantly positive correlation between LV Endo GLS and LV AutoStrain ($r = 0.651$). The slightly more negative values of LV AutoStrain compared to LV Endo GLS may most likely be due to the different analysis methods. In comparison to the published LV GLS average value of -19.7% by Yingchoncharoen et al. [88], this work only showed a slightly less negative LV GLS standard value of -18.19% on visit 1 and an even slightly less negative LV GLS of -17.36% on visit 4. There was no significant difference in LV GLS values between visit 1 and visit 4. Due to the minor differences compared to the reference values and the small study population, the results of this thesis do not provide any further insights into the possible benefits of

strain imaging for the early detection of subclinical systolic dysfunction in hypertensive disease.

4.3 Possible Interactions of Spermidine with the Heart

The supplementation of spermidine, a natural autophagy inducer, is associated with healthful properties against CVD, metabolic disease, and neurodegenerative changes [124,152,153].

Eisenberg et al. [124] already demonstrated the possible cardioprotective effects of dietary spermidine intake in rodent animal models. In this animal study, a significantly extended lifespan could be established in both, mice models fed spermidine for life and those fed late in life. In addition, a maintained diastolic function detected by reduced LV ED pressures and higher LV elasticity was observed in mice. Moreover, improving effects on cardiomyocyte composition and function could be demonstrated, suggesting spermidine has intrinsic properties on cardiomyocytes. This animal study also showed the need for spermidine-induced autophagy for cardioprotective effects. Furthermore, in Dahl salt-sensitive rats an increased intake of spermidine resulted in reduced salt-induced LVH remodeling of the aged heart, lower levels of blood pressure, and a prolonged period until the occurrence of heart failure.

Eisenberg et al. [124] also evaluated the protective effects of spermidine supplementation on CVD and blood pressure in human beings, based on prospective epidemiologic data from the Bruneck study [154]. It could be demonstrated that dietary intake of spermidine correlated inversely with human CVD. Specifically, a higher spermidine intake reduced the risk of fatal heart failure by approximately 40% compared to a lower spermidine intake and spermidine was associated significantly inverse with the plasma level of the biomarker N-terminal pro B-type natriuretic peptide (NT-proBNP). In addition, significantly lower arterial blood pressure was observed in the subjects with high levels of spermidine compared to the subjects with low levels. In contrast, putrescine showed blood pressure increasing properties. Moreover, an inverse correlation between higher spermidine intake and acute coronary heart disease, stroke as well as vascular disease resulting in death could be demonstrated [124].

In addition, Kiechl et al. [61] reported an association between dietary spermidine intake and prolonged survival in human beings in a prospective population-based trial.

These data also indicate the cardioprotective properties of spermidine in human beings. However, the results of this work showed neither structural changes in the human heart function nor reduced arterial blood pressure levels in patients with hypertensive disease and spermidine supplementation, as assessed by various echocardiographic parameters. Given the low concentration of spermidine administered orally, the short period of supplementation, and the small number of subjects included, no other results were to be expected.

4.4 Limitations and Strengths

The main limitations of this study result primarily from its retrospective design and use of postprocessing imaging. Because of the partially low image quality and resulting poor measurement conditions, both the author's manual measurements and semiautomatic border detection for strain analysis were partly difficult to implement. A further limitation of this work represents the low significance of the results due to the small number of measurements of each parameter, which was not only caused by the small number of subjects included, but also by lack of visits and missing single views as well as the poor imaging quality mentioned above. Moreover, it must be considered that this work only compared the baseline values with the values at visit 4 and that therefore 50% of the subjects underwent the washout phase over the second half of the observation period. Another important limitation of this work is that due to the SMARTEST trial still ongoing, only echocardiographic data was used and biometric data could not be included. In addition, no direct group comparison was possible as the subjects were still blinded.

The major strength of this work represents the validity of the performed transthoracic echocardiographic examinations, investigated by experienced cardiologists. Furthermore, for precise post-imaging measurements, the author of this thesis was trained by expert cardiologists for some time until achieving routine and correct measurement values for several sample patients. For this reason, biplane and triplane measurements showed continuously comparable values. Another strength

of this work is that all measurements of all visits were performed twice for accurate results. Moreover, to avoid bias, not all visits from one patient were analyzed consecutively, but the same visits of three patients were always measured one after another.

4.5 Conclusion

The results of this work could not prove the possible cardioprotective effects of the polyamine spermidine on human heart function in subjects with arterial hypertension. Spermidine did not affect any significant changes in volume, linear, and strain parameters. Nevertheless, this study could demonstrate the safety of oral spermidine supplementation concerning the myocardial function in hypertensive patients, assessed by both standard echocardiographic and strain parameters. For the determination of the potential cardioprotective properties of spermidine in human beings and a better understanding of the role of changes in GLS in hypertension disease, further clinical research is necessary.

5 Bibliography

1. Williams B, Mancia G, Spiering W, Agabiti Rosei E, Azizi M, Burnier M, et al. 2018 ESC/ESH Guidelines for the management of arterial hypertension. Eur Heart J. 2018;39(33):3021-104. doi: 10.1093/eurheartj/ehy339.

2. Brașoveanu AM, Cruce R, Mogoantă L, Cârlig V. The Treatment of Arterial Hypertension. Curr Health Sci J. 2019;45(4):358-65. doi: 10.12865/chsj.45.04.03.

3. Chow CK, Teo KK, Rangarajan S, Islam S, Gupta R, Avezum A, et al. Prevalence, awareness, treatment, and control of hypertension in rural and urban communities in high-, middle-, and low-income countries. Jama. 2013;310(9):959-68. doi: 10.1001/jama.2013.184182.

4. Jahrbuch der Gesundheitsstatistik 2021 [Internet]. STATISTIK AUSTRIA; 2023 [cited 2023 Nov 08]. Available from: https://www.statistik.at/fileadmin/user_upload/Gesundheitsstatistik-JB_2021_Web-barrierefrei.pdf.

5. Vasan RS, Beiser A, Seshadri S, Larson MG, Kannel WB, D'Agostino RB, et al. Residual lifetime risk for developing hypertension in middle-aged women and men: The Framingham Heart Study. Jama. 2002;287(8):1003-10. doi: 10.1001/jama.287.8.1003.

6. NCD-RisC. Worldwide trends in blood pressure from 1975 to 2015: a pooled analysis of 1479 population-based measurement studies with 19·1 million participants. Lancet. 2017;389(10064):37-55. doi: 10.1016/s0140-6736(16)31919-5.

7. Kearney PM, Whelton M, Reynolds K, Muntner P, Whelton PK, He J. Global burden of hypertension: analysis of worldwide data. Lancet. 2005;365(9455):217-23. doi: 10.1016/s0140-6736(05)17741-1.

8. Lawes CM, Vander Hoorn S, Rodgers A. Global burden of blood-pressure-related disease, 2001. Lancet. 2008;371(9623):1513-8. doi: 10.1016/s0140-6736(08)60655-8.

9. Forouzanfar MH, Liu P, Roth GA, Ng M, Biryukov S, Marczak L, et al. Global Burden of Hypertension and Systolic Blood Pressure of at Least 110 to 115 mm Hg, 1990-2015. Jama. 2017;317(2):165-82. doi: 10.1001/jama.2016.19043.

10. Hengel FE, Sommer C, Wenzel U. [Arterial Hypertension]. Dtsch Med Wochenschr. 2022;147(7):414-28. doi: 10.1055/a-1577-8663.

11. Hanssen H, Boardman H, Deiseroth A, Moholdt T, Simonenko M, Kränkel N, et al. Personalized exercise prescription in the prevention and treatment of arterial hypertension: a Consensus Document from the European Association of Preventive Cardiology (EAPC) and the ESC Council on Hypertension. Eur J Prev Cardiol. 2022;29(1):205-15. doi: 10.1093/eurjpc/zwaa141.

12. O'Donnell MJ, Xavier D, Liu L, Zhang H, Chin SL, Rao-Melacini P, et al. Risk factors for ischaemic and intracerebral haemorrhagic stroke in 22 countries (the INTERSTROKE study): a case-control study. Lancet. 2010;376(9735):112-23. doi: 10.1016/s0140-6736(10)60834-3.

13. Yusuf S, Hawken S, Ounpuu S, Dans T, Avezum A, Lanas F, et al. Effect of potentially modifiable risk factors associated with myocardial infarction in 52 countries (the INTERHEART study): case-control study. Lancet. 2004;364(9438):937-52. doi: 10.1016/s0140-6736(04)17018-9.

14. Wang C, Yuan Y, Zheng M, Pan A, Wang M, Zhao M, et al. Association of Age of Onset of Hypertension With Cardiovascular Diseases and Mortality. J Am Coll Cardiol. 2020;75(23):2921-30. doi: 10.1016/j.jacc.2020.04.038.

15. Al-Makki A, DiPette D, Whelton PK, Murad MH, Mustafa RA, Acharya S, et al. Hypertension Pharmacological Treatment in Adults: A World Health Organization Guideline Executive Summary. Hypertension. 2022;79(1):293-301. doi: 10.1161/hypertensionaha.121.18192.

16. Banegas JR, López-García E, Dallongeville J, Guallar E, Halcox JP, Borghi C, et al. Achievement of treatment goals for primary prevention of cardiovascular disease in clinical practice across Europe: the EURIKA study. Eur Heart J. 2011;32(17):2143-52. doi: 10.1093/eurheartj/ehr080.

17. National Clinical Guideline Centre. The Clinical Management of Primary Hypertension in Adults: Update of Clinical Guidelines 18 and 34. London: Royal College of Physicians (UK); 2011.

18. Staessen JA, Wang J, Bianchi G, Birkenhäger WH. Essential hypertension. Lancet. 2003;361(9369):1629-41. doi: 10.1016/s0140-6736(03)13302-8.

19. Litwin M, Kułaga Z. Obesity, metabolic syndrome, and primary hypertension. Pediatr Nephrol. 2021;36(4):825-37. doi: 10.1007/s00467-020-04579-3.

20. Litwin M, Niemirska A, Sladowska-Kozlowska J, Wierzbicka A, Janas R, Wawer ZT, et al. Regression of target organ damage in children and adolescents with primary hypertension. Pediatr Nephrol. 2010;25(12):2489-99. doi: 10.1007/s00467-010-1626-7.

21. Charles L, Triscott J, Dobbs B. Secondary Hypertension: Discovering the Underlying Cause. Am Fam Physician. 2017;96(7):453-61.

22. Rimoldi SF, Scherrer U, Messerli FH. Secondary arterial hypertension: when, who, and how to screen? Eur Heart J. 2014;35(19):1245-54. doi: 10.1093/eurheartj/eht534.

23. Chobanian AV, Bakris GL, Black HR, Cushman WC, Green LA, Izzo JL, Jr., et al. Seventh report of the Joint National Committee on Prevention, Detection, Evaluation, and Treatment of High Blood Pressure. Hypertension. 2003;42(6):1206-52. doi: 10.1161/01.HYP.0000107251.49515.c2.

24. Omura M, Saito J, Yamaguchi K, Kakuta Y, Nishikawa T. Prospective study on the prevalence of secondary hypertension among hypertensive patients visiting a general outpatient clinic in Japan. Hypertens Res. 2004;27(3):193-202. doi: 10.1291/hypres.27.193.

25. Börgel J, Springer S, Ghafoor J, Arndt D, Duchna HW, Barthel A, et al. Unrecognized secondary causes of hypertension in patients with hypertensive urgency/emergency: prevalence and co-prevalence. Clin Res Cardiol. 2010;99(8):499-506. doi: 10.1007/s00392-010-0148-4.

26. Asayama K, Ohkubo T, Imai Y. In-office and out-of-office blood pressure measurement. J Hum Hypertens. 2021:1-9. doi: 10.1038/s41371-021-00486-8.

27. Stergiou GS, Palatini P, Asmar R, Bilo G, de la Sierra A, Head G, et al. Blood pressure monitoring: theory and practice. European Society of Hypertension Working Group on Blood Pressure Monitoring and Cardiovascular Variability Teaching Course Proceedings. Blood Press Monit. 2018;23(1):1-8. doi: 10.1097/mbp.0000000000000301.

28. Al Ghorani H, Götzinger F, Böhm M, Mahfoud F. Arterial hypertension - Clinical trials update 2021. Nutr Metab Cardiovasc Dis. 2022;32(1):21-31. doi: 10.1016/j.numecd.2021.09.007.

29. Rabi DM, McBrien KA, Sapir-Pichhadze R, Nakhla M, Ahmed SB, Dumanski SM, et al. Hypertension Canada's 2020 Comprehensive Guidelines for the Prevention, Diagnosis, Risk Assessment, and Treatment of Hypertension in Adults and Children. Can J Cardiol. 2020;36(5):596-624. doi: 10.1016/j.cjca.2020.02.086.

30. Marwick TH, Gillebert TC, Aurigemma G, Chirinos J, Derumeaux G, Galderisi M, et al. Recommendations on the use of echocardiography in adult hypertension: a report from the European Association of Cardiovascular Imaging (EACVI) and the American Society of Echocardiography (ASE)†. Eur Heart J Cardiovasc Imaging. 2015;16(6):577-605. doi: 10.1093/ehjci/jev076.

31. Schillaci G, Battista F, Pucci G. A review of the role of electrocardiography in the diagnosis of left ventricular hypertrophy in hypertension. J Electrocardiol. 2012;45(6):617-23. doi: 10.1016/j.jelectrocard.2012.08.051.

32. Pewsner D, Jüni P, Egger M, Battaglia M, Sundström J, Bachmann LM. Accuracy of electrocardiography in diagnosis of left ventricular hypertrophy in arterial hypertension: systematic review. Bmj. 2007;335(7622):711. doi: 10.1136/bmj.39276.636354.AE.

33. Bacharova L, Schocken D, Estes EH, Strauss D. The role of ECG in the diagnosis of left ventricular hypertrophy. Curr Cardiol Rev. 2014;10(3):257-61. doi: 10.2174/1573403x10666140514103220.

34. Muiesan ML, Salvetti M, Monteduro C, Bonzi B, Paini A, Viola S, et al. Left ventricular concentric geometry during treatment adversely affects cardiovascular prognosis in hypertensive patients. Hypertension. 2004;43(4):731-8. doi: 10.1161/01.HYP.0000121223.44837.de.

35. de Simone G, Izzo R, Chinali M, De Marco M, Casalnuovo G, Rozza F, et al. Does information on systolic and diastolic function improve prediction of a cardiovascular event by left ventricular hypertrophy in arterial hypertension? Hypertension. 2010;56(1):99-104. doi: 10.1161/hypertensionaha.110.150128.

36. de Simone G, Izzo R, Aurigemma GP, De Marco M, Rozza F, Trimarco V, et al. Cardiovascular risk in relation to a new classification of hypertensive left ventricular geometric abnormalities. J Hypertens. 2015;33(4):745-54; discussion 54. doi: 10.1097/hjh.0000000000000477.

37. Bella JN, Palmieri V, Roman MJ, Liu JE, Welty TK, Lee ET, et al. Mitral ratio of peak early to late diastolic filling velocity as a predictor of mortality in middle-aged and elderly adults: the Strong Heart Study. Circulation. 2002;105(16):1928-33. doi: 10.1161/01.cir.0000015076.37047.d9.

38. Chinali M, de Simone G, Roman MJ, Bella JN, Liu JE, Lee ET, et al. Left atrial systolic force and cardiovascular outcome. The Strong Heart Study. Am J Hypertens. 2005;18(12 Pt 1):1570-6; discussion 7. doi: 10.1016/j.amjhyper.2005.05.036.

39. Mancia G, Fagard R, Narkiewicz K, Redón J, Zanchetti A, Böhm M, et al. 2013 ESH/ESC Guidelines for the management of arterial hypertension: the Task Force for the management of arterial hypertension of the European Society of Hypertension (ESH) and of the European Society of Cardiology (ESC). J Hypertens. 2013;31(7):1281-357. doi: 10.1097/01.hjh.0000431740.32696.cc.

40. Piepoli MF, Hoes AW, Agewall S, Albus C, Brotons C, Catapano AL, et al. 2016 European Guidelines on cardiovascular disease prevention in clinical practice: The Sixth Joint Task Force of the European Society of Cardiology and Other Societies on Cardiovascular Disease Prevention in Clinical Practice (constituted by representatives of 10 societies and by invited experts) Developed with the special contribution of the European Association for Cardiovascular Prevention & Rehabilitation (EACPR). Eur Heart J. 2016;37(29):2315-81. doi: 10.1093/eurheartj/ehw106.

41. He FJ, Li J, Macgregor GA. Effect of longer term modest salt reduction on blood pressure: Cochrane systematic review and meta-analysis of randomised trials. Bmj. 2013;346:f1325. doi: 10.1136/bmj.f1325.

42. Graudal NA, Hubeck-Graudal T, Jürgens G. Effects of low-sodium diet vs. high-sodium diet on blood pressure, renin, aldosterone, catecholamines, cholesterol, and triglyceride (Cochrane Review). Am J Hypertens. 2012;25(1):1-15. doi: 10.1038/ajh.2011.210.

43. Schillaci G, Pucci G. Regression of coronary microvascular changes: the role of blood pressure-lowering treatment. Am J Hypertens. 2011;24(4):381-2. doi: 10.1038/ajh.2011.11.

44. Aburto NJ, Ziolkovska A, Hooper L, Elliott P, Cappuccio FP, Meerpohl JJ. Effect of lower sodium intake on health: systematic review and meta-analyses. Bmj. 2013;346:f1326. doi: 10.1136/bmj.f1326.

45. Frisoli TM, Schmieder RE, Grodzicki T, Messerli FH. Beyond salt: lifestyle modifications and blood pressure. Eur Heart J. 2011;32(24):3081-7. doi: 10.1093/eurheartj/ehr379.

46. Holmes MV, Dale CE, Zuccolo L, Silverwood RJ, Guo Y, Ye Z, et al. Association between alcohol and cardiovascular disease: Mendelian randomisation analysis based on individual participant data. Bmj. 2014;349:g4164. doi: 10.1136/bmj.g4164.

47. Samadian F, Dalili N, Jamalian A. Lifestyle Modifications to Prevent and Control Hypertension. Iran J Kidney Dis. 2016;10(5):237-63.

48. Daskalopoulou SS, Rabi DM, Zarnke KB, Dasgupta K, Nerenberg K, Cloutier L, et al. The 2015 Canadian Hypertension Education Program recommendations for blood pressure measurement, diagnosis, assessment of risk, prevention, and treatment of hypertension. Can J Cardiol. 2015;31(5):549-68. doi: 10.1016/j.cjca.2015.02.016.

49. Kjeldsen S, Feldman RD, Lisheng L, Mourad JJ, Chiang CE, Zhang W, et al. Updated national and international hypertension guidelines: a review of current recommendations. Drugs. 2014;74(17):2033-51. doi: 10.1007/s40265-014-0306-5.

50. Gradman AH, Basile JN, Carter BL, Bakris GL. Combination therapy in hypertension. J Am Soc Hypertens. 2010;4(1):42-50. doi: 10.1016/j.jash.2010.02.005.

51. Ettehad D, Emdin CA, Kiran A, Anderson SG, Callender T, Emberson J, et al. Blood pressure lowering for prevention of cardiovascular disease and death: a systematic review and meta-analysis. Lancet. 2016;387(10022):957-67. doi: 10.1016/s0140-6736(15)01225-8.

52. Beckett N, Peters R, Leonetti G, Duggan J, Fagard R, Thijs L, et al. Subgroup and per-protocol analyses from the Hypertension in the Very Elderly Trial. J Hypertens. 2014;32(7):1478-87; discussion 87. doi: 10.1097/hjh.0000000000000195.

53. Kurihara S. Polyamine metabolism and transport in gut microbes. Biosci Biotechnol Biochem. 2022;86(8):957-66. doi: 10.1093/bbb/zbac080.

54. Igarashi K, Kashiwagi K. Modulation of cellular function by polyamines. Int J Biochem Cell Biol. 2010;42(1):39-51. doi: 10.1016/j.biocel.2009.07.009.

55. Igarashi K, Kashiwagi K. Polyamines: mysterious modulators of cellular functions. Biochem Biophys Res Commun. 2000;271(3):559-64. doi: 10.1006/bbrc.2000.2601.

56. Pegg AE. Mammalian polyamine metabolism and function. IUBMB Life. 2009;61(9):880-94. doi: 10.1002/iub.230.

57. Landau G, Bercovich Z, Park MH, Kahana C. The role of polyamines in supporting growth of mammalian cells is mediated through their requirement for translation initiation and elongation. J Biol Chem. 2010;285(17):12474-81. doi: 10.1074/jbc.M110.106419.

58. Williams K. Interactions of polyamines with ion channels. Biochem J. 1997;325 (Pt 2)(Pt 2):289-97. doi: 10.1042/bj3250289.

59. Ghosh I, Sankhe R, Mudgal J, Arora D, Nampoothiri M. Spermidine, an autophagy inducer, as a therapeutic strategy in neurological disorders. Neuropeptides. 2020;83:102083. doi: 10.1016/j.npep.2020.102083.

60. Bachrach U. The early history of polyamine research. Plant Physiol Biochem. 2010;48(7):490-5. doi: 10.1016/j.plaphy.2010.02.003.

61. Kiechl S, Pechlaner R, Willeit P, Notdurfter M, Paulweber B, Willeit K, et al. Higher spermidine intake is linked to lower mortality: a prospective population-based study. Am J Clin Nutr. 2018;108(2):371-80. doi: 10.1093/ajcn/nqy102.

62. Atiya Ali M, Poortvliet E, Strömberg R, Yngve A. Polyamines in foods: development of a food database. Food Nutr Res. 2011;55. doi: 10.3402/fnr.v55i0.5572.

63. Scalabrino G, Ferioli ME. Polyamines in mammalian ageing: an oncological problem, too? A review. Mech Ageing Dev. 1984;26(2-3):149-64. doi: 10.1016/0047-6374(84)90090-3.

64. Eisenberg T, Knauer H, Schauer A, Büttner S, Ruckenstuhl C, Carmona-Gutierrez D, et al. Induction of autophagy by spermidine promotes longevity. Nat Cell Biol. 2009;11(11):1305-14. doi: 10.1038/ncb1975.

65. Mandal S, Mandal A, Johansson HE, Orjalo AV, Park MH. Depletion of cellular polyamines, spermidine and spermine, causes a total arrest in translation and growth in mammalian cells. Proc Natl Acad Sci U S A. 2013;110(6):2169-74. doi: 10.1073/pnas.1219002110.

66. Đorđievski S, Vukašinović EL, Čelić TV, Pihler I, Kebert M, Kojić D, et al. Spermidine dietary supplementation and polyamines level in reference to survival and lifespan of honey bees. Sci Rep. 2023;13(1):4329. doi: 10.1038/s41598-023-31456-4.

67. Voigt JU, Cvijic M. 2- and 3-Dimensional Myocardial Strain in Cardiac Health and Disease. JACC Cardiovasc Imaging. 2019;12(9):1849-63. doi: 10.1016/j.jcmg.2019.01.044.

68. Pavlopoulos H, Nihoyannopoulos P. Strain and strain rate deformation parameters: from tissue Doppler to 2D speckle tracking. Int J Cardiovasc Imaging. 2008;24(5):479-91. doi: 10.1007/s10554-007-9286-9.

69. Voigt JU, Pedrizzetti G, Lysyansky P, Marwick TH, Houle H, Baumann R, et al. Definitions for a common standard for 2D speckle tracking echocardiography: consensus document of the EACVI/ASE/Industry Task Force to standardize deformation imaging. Eur Heart J Cardiovasc Imaging. 2015;16(1):1-11. doi: 10.1093/ehjci/jeu184.

70. Johnson C, Kuyt K, Oxborough D, Stout M. Practical tips and tricks in measuring strain, strain rate and twist for the left and right ventricles. Echo Res Pract. 2019;6(3):R87-r98. doi: 10.1530/erp-19-0020.

71. Urheim S, Edvardsen T, Torp H, Angelsen B, Smiseth OA. Myocardial strain by Doppler echocardiography. Validation of a new method to quantify regional myocardial function. Circulation. 2000;102(10):1158-64. doi: 10.1161/01.cir.102.10.1158.

72. Hoit BD. Strain and strain rate echocardiography and coronary artery disease. Circ Cardiovasc Imaging. 2011;4(2):179-90. doi: 10.1161/circimaging.110.959817.

73. Mor-Avi V, Lang RM, Badano LP, Belohlavek M, Cardim NM, Derumeaux G, et al. Current and evolving echocardiographic techniques for the quantitative evaluation of cardiac mechanics: ASE/EAE consensus statement on methodology and indications endorsed by the Japanese Society of Echocardiography. J Am Soc Echocardiogr. 2011;24(3):277-313. doi: 10.1016/j.echo.2011.01.015.

74. Abraham TP, Dimaano VL, Liang HY. Role of tissue Doppler and strain echocardiography in current clinical practice. Circulation. 2007;116(22):2597-609. doi: 10.1161/circulationaha.106.647172.

75. Pellerin D, Sharma R, Elliott P, Veyrat C. Tissue Doppler, strain, and strain rate echocardiography for the assessment of left and right systolic ventricular function. Heart. 2003;89 Suppl 3(Suppl 3):iii9-17. doi: 10.1136/heart.89.suppl_3.iii9.

76. Dandel M, Lehmkuhl H, Knosalla C, Suramelashvili N, Hetzer R. Strain and strain rate imaging by echocardiography - basic concepts and clinical applicability. Curr Cardiol Rev. 2009;5(2):133-48. doi: 10.2174/157340309788166642.

77. Lancellotti P, Cosyns B, Zacharakis D, Attena E, Van Camp G, Gach O, et al. Importance of left ventricular longitudinal function and functional reserve in patients with degenerative mitral regurgitation: assessment by two-dimensional speckle tracking. J Am Soc Echocardiogr. 2008;21(12):1331-6. doi: 10.1016/j.echo.2008.09.023.

78. Geyer H, Caracciolo G, Abe H, Wilansky S, Carerj S, Gentile F, et al. Assessment of myocardial mechanics using speckle tracking echocardiography: fundamentals and clinical applications. J Am Soc Echocardiogr. 2010;23(4):351-69; quiz 453-5. doi: 10.1016/j.echo.2010.02.015.

79. Helle-Valle T, Crosby J, Edvardsen T, Lyseggen E, Amundsen BH, Smith HJ, et al. New noninvasive method for assessment of left ventricular rotation: speckle tracking echocardiography. Circulation. 2005;112(20):3149-56. doi: 10.1161/circulationaha.104.531558.

80. Teske AJ, De Boeck BW, Melman PG, Sieswerda GT, Doevendans PA, Cramer MJ. Echocardiographic quantification of myocardial function using tissue deformation imaging, a guide to image acquisition and analysis using tissue Doppler and speckle tracking. Cardiovasc Ultrasound. 2007;5:27. doi: 10.1186/1476-7120-5-27.

81. Rademakers FE, Rogers WJ, Guier WH, Hutchins GM, Siu CO, Weisfeldt ML, et al. Relation of regional cross-fiber shortening to wall thickening in the intact heart. Three-dimensional strain analysis by NMR tagging. Circulation. 1994;89(3):1174-82. doi: 10.1161/01.cir.89.3.1174.

82. Salerno M. Feature Tracking by CMR: A "Double Feature"? JACC Cardiovasc Imaging. 2018;11(2 Pt 1):206-8. doi: 10.1016/j.jcmg.2017.01.024.

83. Cerqueira MD, Weissman NJ, Dilsizian V, Jacobs AK, Kaul S, Laskey WK, et al. Standardized myocardial segmentation and nomenclature for tomographic imaging of the heart. A statement for healthcare professionals from the Cardiac Imaging Committee of the Council on Clinical Cardiology of the American Heart Association. Circulation. 2002;105(4):539-42. doi: 10.1161/hc0402.102975.

84. Lang RM, Badano LP, Mor-Avi V, Afilalo J, Armstrong A, Ernande L, et al. Recommendations for cardiac chamber quantification by echocardiography in adults: an update from the American Society of Echocardiography and the European Association of Cardiovascular Imaging. Eur Heart J Cardiovasc Imaging. 2015;16(3):233-70. doi: 10.1093/ehjci/jev014.

85. Sarvari SI, Haugaa KH, Zahid W, Bendz B, Aakhus S, Aaberge L, et al. Layer-specific quantification of myocardial deformation by strain echocardiography may reveal significant CAD in patients with non-ST-segment elevation acute coronary syndrome. JACC Cardiovasc Imaging. 2013;6(5):535-44. doi: 10.1016/j.jcmg.2013.01.009.

86. Ünlü S, Mirea O, Duchenne J, Pagourelias ED, Bézy S, Thomas JD, et al. Comparison of Feasibility, Accuracy, and Reproducibility of Layer-Specific Global Longitudinal Strain Measurements Among Five Different Vendors: A Report from the EACVI-ASE Strain Standardization Task Force. J Am Soc Echocardiogr. 2018;31(3):374-80.e1. doi: 10.1016/j.echo.2017.11.008.

87. Marwick TH, Leano RL, Brown J, Sun JP, Hoffmann R, Lysyansky P, et al. Myocardial strain measurement with 2-dimensional speckle-tracking echocardiography: definition of normal range. JACC Cardiovasc Imaging. 2009;2(1):80-4. doi: 10.1016/j.jcmg.2007.12.007.

88. Yingchoncharoen T, Agarwal S, Popović ZB, Marwick TH. Normal ranges of left ventricular strain: a meta-analysis. J Am Soc Echocardiogr. 2013;26(2):185-91. doi: 10.1016/j.echo.2012.10.008.

89. Sugimoto T, Dulgheru R, Bernard A, Ilardi F, Contu L, Addetia K, et al. Echocardiographic reference ranges for normal left ventricular 2D strain: results from the EACVI NORRE study. Eur Heart J Cardiovasc Imaging. 2017;18(8):833-40. doi: 10.1093/ehjci/jex140.

90. Takigiku K, Takeuchi M, Izumi C, Yuda S, Sakata K, Ohte N, et al. Normal range of left ventricular 2-dimensional strain: Japanese Ultrasound Speckle Tracking of the Left Ventricle (JUSTICE) study. Circ J. 2012;76(11):2623-32. doi: 10.1253/circj.cj-12-0264.

91. Kocabay G, Muraru D, Peluso D, Cucchini U, Mihaila S, Padayattil-Jose S, et al. Normal left ventricular mechanics by two-dimensional speckle-tracking echocardiography. Reference values in healthy adults. Rev Esp Cardiol (Engl Ed). 2014;67(8):651-8. doi: 10.1016/j.rec.2013.12.009.

92. Kuznetsova T, Herbots L, Richart T, D'Hooge J, Thijs L, Fagard RH, et al. Left ventricular strain and strain rate in a general population. Eur Heart J. 2008;29(16):2014-23. doi: 10.1093/eurheartj/ehn280.

93. Weidemann F, Jamal F, Sutherland GR, Claus P, Kowalski M, Hatle L, et al. Myocardial function defined by strain rate and strain during alterations in inotropic states and heart rate. Am J Physiol Heart Circ Physiol. 2002;283(2):H792-9. doi: 10.1152/ajpheart.00025.2002.

94. Dahle GO, Stangeland L, Moen CA, Salminen PR, Haaverstad R, Matre K, et al. The influence of acute unloading on left ventricular strain and strain rate by speckle tracking echocardiography in a porcine model. Am J Physiol Heart Circ Physiol. 2016;310(10):H1330-9. doi: 10.1152/ajpheart.00947.2015.

95. Donal E, Bergerot C, Thibault H, Ernande L, Loufoua J, Augeul L, et al. Influence of afterload on left ventricular radial and longitudinal systolic functions: a two-dimensional strain imaging study. Eur J Echocardiogr. 2009;10(8):914-21. doi: 10.1093/ejechocard/jep095.

96. Galderisi M, Lomoriello VS, Santoro A, Esposito R, Olibet M, Raia R, et al. Differences of myocardial systolic deformation and correlates of diastolic function in competitive rowers and young hypertensives: a speckle-tracking echocardiography study. J Am Soc Echocardiogr. 2010;23(11):1190-8. doi: 10.1016/j.echo.2010.07.010.

97. Carasso S, Cohen O, Mutlak D, Adler Z, Lessick J, Aronson D, et al. Relation of myocardial mechanics in severe aortic stenosis to left ventricular ejection fraction and response to aortic valve replacement. Am J Cardiol. 2011;107(7):1052-7. doi: 10.1016/j.amjcard.2010.11.032.

98. Shiels HA, White E. The Frank-Starling mechanism in vertebrate cardiac myocytes. J Exp Biol. 2008;211(Pt 13):2005-13. doi: 10.1242/jeb.003145.

99. Kim HM, Cho GY, Hwang IC, Choi HM, Park JB, Yoon YE, et al. Myocardial Strain in Prediction of Outcomes After Surgery for Severe Mitral Regurgitation. JACC Cardiovasc Imaging. 2018;11(9):1235-44. doi: 10.1016/j.jcmg.2018.03.016.

100. Marciniak A, Claus P, Sutherland GR, Marciniak M, Karu T, Baltabaeva A, et al. Changes in systolic left ventricular function in isolated mitral regurgitation. A strain rate imaging study. Eur Heart J. 2007;28(21):2627-36. doi: 10.1093/eurheartj/ehm072.

101. Mentias A, Naji P, Gillinov AM, Rodriguez LL, Reed G, Mihaljevic T, et al. Strain Echocardiography and Functional Capacity in Asymptomatic Primary Mitral Regurgitation With Preserved Ejection Fraction. J Am Coll Cardiol. 2016;68(18):1974-86. doi: 10.1016/j.jacc.2016.08.030.

102. Marciniak A, Sutherland GR, Marciniak M, Claus P, Bijnens B, Jahangiri M. Myocardial deformation abnormalities in patients with aortic regurgitation: a strain rate imaging study. Eur J Echocardiogr. 2009;10(1):112-9. doi: 10.1093/ejechocard/jen185.

103. Smedsrud MK, Pettersen E, Gjesdal O, Svennevig JL, Andersen K, Ihlen H, et al. Detection of left ventricular dysfunction by global longitudinal systolic strain in patients with chronic aortic regurgitation. J Am Soc Echocardiogr. 2011;24(11):1253-9. doi: 10.1016/j.echo.2011.08.003.

104. Reant P, Metras A, Detaille D, Reynaud A, Diolez P, Jaspard-Vinassa B, et al. Impact of Afterload Increase on Left Ventricular Myocardial Deformation Indices. J Am Soc Echocardiogr. 2016;29(12):1217-28. doi: 10.1016/j.echo.2016.09.006.

105. Rost C, Rost MC, Breithardt OA, Schmid M, Klinghammer L, Stumpf C, et al. Relation of functional echocardiographic parameters to infarct scar transmurality by magnetic resonance imaging. J Am Soc Echocardiogr. 2014;27(7):767-74. doi: 10.1016/j.echo.2014.02.004.

106. Ternacle J, Bodez D, Guellich A, Audureau E, Rappeneau S, Lim P, et al. Causes and Consequences of Longitudinal LV Dysfunction Assessed by 2D Strain Echocardiography in Cardiac Amyloidosis. JACC Cardiovasc Imaging. 2016;9(2):126-38. doi: 10.1016/j.jcmg.2015.05.014.

107. Phelan D, Collier P, Thavendiranathan P, Popović ZB, Hanna M, Plana JC, et al. Relative apical sparing of longitudinal strain using two-dimensional speckle-tracking echocardiography is both sensitive and specific for the diagnosis of cardiac amyloidosis. Heart. 2012;98(19):1442-8. doi: 10.1136/heartjnl-2012-302353.

108. Mada RO, Lysyansky P, Daraban AM, Duchenne J, Voigt JU. How to define end-diastole and end-systole?: Impact of timing on strain measurements. JACC Cardiovasc Imaging. 2015;8(2):148-57. doi: 10.1016/j.jcmg.2014.10.010.

109. Kosaraju A, Goyal A, Grigorova Y, Makaryus AN. Left Ventricular Ejection Fraction. 2023. In: StatPearls [Internet]. Treasure Island (FL): StatPearls Publishing; 2024.

110. Naser N, Stankovic I, Neskovic A. The Reliability of Automated Three-Dimensional Echocardiography-HeartModel(A.I.) Versus 2D Echocardiography Simpson Methods in Evaluation of Left Ventricle Volumes and Ejection Fraction in Patients With Left Ventricular Dysfunction. Med Arch. 2022;76(4):259-66. doi: 10.5455/medarh.2022.76.259-266.

111. Stokke TM, Hasselberg NE, Smedsrud MK, Sarvari SI, Haugaa KH, Smiseth OA, et al. Geometry as a Confounder When Assessing Ventricular Systolic Function: Comparison Between Ejection Fraction and Strain. J Am Coll Cardiol. 2017;70(8):942-54. doi: 10.1016/j.jacc.2017.06.046.

112. Lumens J, Prinzen FW, Delhaas T. Longitudinal Strain: "Think Globally, Track Locally". JACC Cardiovasc Imaging. 2015;8(12):1360-3. doi: 10.1016/j.jcmg.2015.08.014.

113. Kalam K, Otahal P, Marwick TH. Prognostic implications of global LV dysfunction: a systematic review and meta-analysis of global longitudinal strain and ejection fraction. Heart. 2014;100(21):1673-80. doi: 10.1136/heartjnl-2014-305538.

114. Thavendiranathan P, Poulin F, Lim KD, Plana JC, Woo A, Marwick TH. Use of myocardial strain imaging by echocardiography for the early detection of cardiotoxicity in patients during and after cancer chemotherapy: a systematic review. J Am Coll Cardiol. 2014;63(25 Pt A):2751-68. doi: 10.1016/j.jacc.2014.01.073.

115. Zamorano JL, Lancellotti P, Rodriguez Muñoz D, Aboyans V, Asteggiano R, Galderisi M, et al. 2016 ESC Position Paper on cancer treatments and cardiovascular toxicity developed under the auspices of the ESC Committee for Practice Guidelines: The Task Force for cancer treatments and cardiovascular toxicity of the European Society of Cardiology (ESC). Eur Heart J. 2016;37(36):2768-801. doi: 10.1093/eurheartj/ehw211.

116. Sawaya H, Sebag IA, Plana JC, Januzzi JL, Ky B, Tan TC, et al. Assessment of echocardiography and biomarkers for the extended prediction of cardiotoxicity in patients treated with anthracyclines, taxanes, and trastuzumab. Circ Cardiovasc Imaging. 2012;5(5):596-603. doi: 10.1161/circimaging.112.973321.

117. Alashi A, Mentias A, Abdallah A, Feng K, Gillinov AM, Rodriguez LL, et al. Incremental Prognostic Utility of Left Ventricular Global Longitudinal Strain in Asymptomatic Patients With Significant Chronic Aortic Regurgitation and Preserved Left Ventricular Ejection Fraction. JACC Cardiovasc Imaging. 2018;11(5):673-82. doi: 10.1016/j.jcmg.2017.02.016.

118. Holland DJ, Marwick TH, Haluska BA, Leano R, Hordern MD, Hare JL, et al. Subclinical LV dysfunction and 10-year outcomes in type 2 diabetes mellitus. Heart. 2015;101(13):1061-6. doi: 10.1136/heartjnl-2014-307391.

119. Rovner A, de las Fuentes L, Waggoner AD, Memon N, Chohan R, Dávila-Román VG. Characterization of left ventricular diastolic function in hypertension by use of Doppler tissue imaging and color M-mode techniques. J Am Soc Echocardiogr. 2006;19(7):872-9. doi: 10.1016/j.echo.2006.01.023.

120. Edvardsen T, Rosen BD, Pan L, Jerosch-Herold M, Lai S, Hundley WG, et al. Regional diastolic dysfunction in individuals with left ventricular hypertrophy measured by tagged magnetic resonance imaging--the Multi-Ethnic Study of Atherosclerosis (MESA). Am Heart J. 2006;151(1):109-14. doi: 10.1016/j.ahj.2005.02.018.

121. Imbalzano E, Zito C, Carerj S, Oreto G, Mandraffino G, Cusmà-Piccione M, et al. Left ventricular function in hypertension: new insight by speckle tracking echocardiography. Echocardiography. 2011;28(6):649-57. doi: 10.1111/j.1540-8175.2011.01410.x.

122. Galderisi M, Trimarco B. Global longitudinal strain: a novel hallmark of cardiac risk in arterial hypertension. J Hypertens. 2016;34(6):1050-1. doi: 10.1097/hjh.0000000000000920.

123. Leitman M, Lysyansky P, Sidenko S, Shir V, Peleg E, Binenbaum M, et al. Two-dimensional strain-a novel software for real-time quantitative echocardiographic assessment of myocardial function. J Am Soc Echocardiogr. 2004;17(10):1021-9. doi: 10.1016/j.echo.2004.06.019.

124. Eisenberg T, Abdellatif M, Schroeder S, Primessnig U, Stekovic S, Pendl T, et al. Cardioprotection and lifespan extension by the natural polyamine spermidine. Nat Med. 2016;22(12):1428-38. doi: 10.1038/nm.4222.

125. Field A. Discovering statistics using SPSS. 3 ed. SAGE Publications 2009.

126. Cohen J. Set correlation and contingency tables. Applied Psychological Measurement. . 1988;12(4):425-34. doi: 10.1177/014662168801200410.

127. Reichek N, Helak J, Plappert T, Sutton MS, Weber KT. Anatomic validation of left ventricular mass estimates from clinical two-dimensional echocardiography: initial results. Circulation. 1983;67(2):348-52. doi: 10.1161/01.cir.67.2.348.

128. Devereux RB, Reichek N. Echocardiographic determination of left ventricular mass in man. Anatomic validation of the method. Circulation. 1977;55(4):613-8. doi: 10.1161/01.cir.55.4.613.

129. Woythaler JN, Singer SL, Kwan OL, Meltzer RS, Reubner B, Bommer W, et al. Accuracy of echocardiography versus electrocardiography in detecting left ventricular hypertrophy: comparison with postmortem mass measurements. J Am Coll Cardiol. 1983;2(2):305-11. doi: 10.1016/s0735-1097(83)80167-3.

130. Koren MJ, Devereux RB, Casale PN, Savage DD, Laragh JH. Relation of left ventricular mass and geometry to morbidity and mortality in uncomplicated essential hypertension. Ann Intern Med. 1991;114(5):345-52. doi: 10.7326/0003-4819-114-5-345.

131. Verdecchia P, Porcellati C, Reboldi G, Gattobigio R, Borgioni C, Pearson TA, et al. Left ventricular hypertrophy as an independent predictor of acute cerebrovascular events in essential hypertension. Circulation. 2001;104(17):2039-44. doi: 10.1161/hc4201.097944.

132. Levy D. Left ventricular hypertrophy. Epidemiological insights from the Framingham Heart Study. Drugs. 1988;35 Suppl 5:1-5. doi: 10.2165/00003495-198800355-00002.

133. Levy D, Garrison RJ, Savage DD, Kannel WB, Castelli WP. Left ventricular mass and incidence of coronary heart disease in an elderly cohort. The Framingham Heart Study. Ann Intern Med. 1989;110(2):101-7. doi: 10.7326/0003-4819-110-2-101.

134. Levy D, Garrison RJ, Savage DD, Kannel WB, Castelli WP. Prognostic implications of echocardiographically determined left ventricular mass in the Framingham Heart Study. N Engl J Med. 1990;322(22):1561-6. doi: 10.1056/nejm199005313222203.

135. Casale PN, Devereux RB, Milner M, Zullo G, Harshfield GA, Pickering TG, et al. Value of echocardiographic measurement of left ventricular mass in predicting cardiovascular morbid events in hypertensive men. Ann Intern Med. 1986;105(2):173-8. doi: 10.7326/0003-4819-105-2-173.

136. Devereux RB, Wachtell K, Gerdts E, Boman K, Nieminen MS, Papademetriou V, et al. Prognostic significance of left ventricular mass change during treatment of hypertension. Jama. 2004;292(19):2350-6. doi: 10.1001/jama.292.19.2350.

137. Verdecchia P, Angeli F, Borgioni C, Gattobigio R, de Simone G, Devereux RB, et al. Changes in cardiovascular risk by reduction of left ventricular mass in hypertension: a meta-analysis. Am J Hypertens. 2003;16(11 Pt 1):895-9. doi: 10.1016/s0895-7061(03)01018-5.

138. de Simone G, Devereux RB, Celentano A, Roman MJ. Left ventricular chamber and wall mechanics in the presence of concentric geometry. J Hypertens. 1999;17(7):1001-6. doi: 10.1097/00004872-199917070-00017.

139. Potter E, Marwick TH. Assessment of Left Ventricular Function by Echocardiography: The Case for Routinely Adding Global Longitudinal Strain to Ejection Fraction. JACC Cardiovasc Imaging. 2018;11(2 Pt 1):260-74. doi: 10.1016/j.jcmg.2017.11.017.

140. Nagueh SF, Appleton CP, Gillebert TC, Marino PN, Oh JK, Smiseth OA, et al. Recommendations for the evaluation of left ventricular diastolic function by echocardiography. J Am Soc Echocardiogr. 2009;22(2):107-33. doi: 10.1016/j.echo.2008.11.023.

141. Fouad FM, Slominski JM, Tarazi RC. Left ventricular diastolic function in hypertension: relation to left ventricular mass and systolic function. J Am Coll Cardiol. 1984;3(6):1500-6. doi: 10.1016/s0735-1097(84)80289-2.

142. Messerli FH, Rimoldi SF, Bangalore S. The Transition From Hypertension to Heart Failure: Contemporary Update. JACC Heart Fail. 2017;5(8):543-51. doi: 10.1016/j.jchf.2017.04.012.

143. Fouad FM, Tarazi RC, Gallagher JH, MacIntyre WJ, Cook SA. Abnormal left ventricular relaxation in hypertensive patients. Clin Sci (Lond). 1980;59 Suppl 6:411s-4s. doi: 10.1042/cs059411s.

144. Lam CS, Lyass A, Kraigher-Krainer E, Massaro JM, Lee DS, Ho JE, et al. Cardiac dysfunction and noncardiac dysfunction as precursors of heart failure with reduced and preserved ejection fraction in the community. Circulation. 2011;124(1):24-30. doi: 10.1161/circulationaha.110.979203.

145. Kane GC, Karon BL, Mahoney DW, Redfield MM, Roger VL, Burnett JC, Jr., et al. Progression of left ventricular diastolic dysfunction and risk of heart failure. Jama. 2011;306(8):856-63. doi: 10.1001/jama.2011.1201.

146. Nagueh SF. Left Ventricular Diastolic Function: Understanding Pathophysiology, Diagnosis, and Prognosis With Echocardiography. JACC Cardiovasc Imaging. 2020;13(1 Pt 2):228-44. doi: 10.1016/j.jcmg.2018.10.038.

147. Nagueh SF, Smiseth OA, Appleton CP, Byrd BF, 3rd, Dokainish H, Edvardsen T, et al. Recommendations for the Evaluation of Left Ventricular Diastolic Function by Echocardiography: An Update from the American Society of Echocardiography and the European Association of Cardiovascular Imaging. J Am Soc Echocardiogr. 2016;29(4):277-314. doi: 10.1016/j.echo.2016.01.011.

148. Schillaci G, Pasqualini L, Verdecchia P, Vaudo G, Marchesi S, Porcellati C, et al. Prognostic significance of left ventricular diastolic dysfunction in essential hypertension. J Am Coll Cardiol. 2002;39(12):2005-11. doi: 10.1016/s0735-1097(02)01896-x.

149. Gonçalves S, Cortez-Dias N, Nunes A, Belo A, Zimbarra Cabrita I, Sousa C, et al. Left ventricular systolic dysfunction detected by speckle tracking in hypertensive patients with preserved ejection fraction. Rev Port Cardiol. 2014;33(1):27-37. doi: 10.1016/j.repc.2013.07.009.

150. Kosmala W, Plaksej R, Strotmann JM, Weigel C, Herrmann S, Niemann M, et al. Progression of left ventricular functional abnormalities in hypertensive patients with heart failure: an ultrasonic two-dimensional speckle tracking study. J Am Soc Echocardiogr. 2008;21(12):1309-17. doi: 10.1016/j.echo.2008.10.006.

151. Sengupta SP, Caracciolo G, Thompson C, Abe H, Sengupta PP. Early impairment of left ventricular function in patients with systemic hypertension: new insights with 2-dimensional speckle tracking echocardiography. Indian Heart J. 2013;65(1):48-52. doi: 10.1016/j.ihj.2012.12.009.

152. Madeo F, Eisenberg T, Pietrocola F, Kroemer G. Spermidine in health and disease. Science. 2018;359(6374). doi: 10.1126/science.aan2788.

153. Freitag K, Sterczyk N, Wendlinger S, Obermayer B, Schulz J, Farztdinov V, et al. Spermidine reduces neuroinflammation and soluble amyloid beta in an Alzheimer's disease mouse model. J Neuroinflammation. 2022;19(1):172. doi: 10.1186/s12974-022-02534-7.

154. Stegemann C, Pechlaner R, Willeit P, Langley SR, Mangino M, Mayr U, et al. Lipidomics profiling and risk of cardiovascular disease in the prospective population-based Bruneck study. Circulation. 2014;129(18):1821-31. doi: 10.1161/circulationaha.113.002500.